Mafic dykes as monitors of hp granulite facies metamorphism in the Grenville front tectonic zone (western Quebec)

Jacques Martignole, Jean-Emmanuel Martelat

MAFIC DYKES AS MONITORS OF HP GRANULITE FACIES METAMORPHISM IN THE GRENVILLE FRONT TECTONIC ZONE (WESTERN QUEBEC)

Jacques Martignole and Jean-Emmanuel Martelat*

Département de géologie, Université de Montréal
CP 6128, Montréal, H3C 3J7, Qc, Canada
*Laboratoire de Géodynamique des Chaînes Alpines (UMR 5025)
BP 53, 38041,Grenoble Cedex, France

Abstract

In the Grenville Province of western Quebec, Archean gneisses and Paleo- to Mesoproterozoic dykes have been reworked during a short-lived high-pressure metamorphic event at about 1.0 Ga. To the SE of the Grenville Front, a SE-dipping 30 km-thick slab of quartzofeldspathic granulites and biotite-garnet (±opx) gneisses overrides, along the McLaurin thrust, a 4 km-thick zone of steeply dipping muscovite-sillimanite micaschists that abuts on the Grenville Front. The granulitic slab in turn dips under amphibolite-grade migmatites, along the Dorval detachment. The micaschists, the granulites, the biotite-garnet gneisses, and the migmatites are of Archean provenance (Sm-Nd model ages) and correspond to the Grenvillian parautochthon. Metamorphosed mafic dykes are found to intersect at several localities the gneissic foliation of these rocks. Pods of coronitic metagabbros are also found in the same area. New U-Th-Pb chemical ages on monazite from the host rocks support previous estimations of ca. 2.7 Ga for the Archean metamorphism and 1.0 Ga for the Grenvillian reworking. As these determinations failed to recognize intermediate ages, it is likely that Proterozoic mafic dykes and pods are truly monocyclic, i.e. they only went through the Grenvillian metamorphic event. Metamorphic dykes have preserved fine-grained chilled margins, igneous fabrics, magmatic layering and Fe-Ti-rich, Si-poor chemistry in spite of a strong overprint attested by various types of reaction rims (coronitic structures). The coronitic gabbros lack magmatic fabrics and have a more primitive composition with higher Mg-number and normative quartz. In metamorphosed mafic dykes of the granulite slab, large pyroxenes are rimmed by garnet coronas with minute quartz inclusions, suggesting the reaction pl+opx = grt+qtz. Garnet coronas, in turn, are locally replaced by symplectites of opx, hbl, pl and qtz, probably formed through back reactions grt+cpx+qtz = pl+opx and grt+cpx = hbl+qtz. Thermobarometric calculations using the above assemblages indicate peak equilibration at

about 1.2-1.4 GPa at temperatures of about 800°C followed by a quasi-isothermal decompression in the vicinity of 0.9 MPa at temperatures around 700°C.
Cross-cutting relationships and the persistence of magmatic fabrics within the dykes of the granulitic slab suggest emplacement in a brittle extensional setting whereas garnet coronas attest to subsequent burial under high-pressure (HP) granulite facies at relatively high temperature. As it is likely that some of the metamorphosed dykes belong to the 1.14 Ga-old Abitibi swarm, Grenvillian HP granulite metamorphism would corresponds to burial of upper crustal levels down to sub-Moho depths with concomitant heating, followed by rapid exhumation. This situation is reminiscent of the emplacement-deformation-exhumation history of the SE-striking 1240 Ma-old Sudbury dyke swarm in Ontario (Bethune, 1997) and may be a characteristic of the Grenville Front Tectonic Zone.

Keywords: Grenville Province, mafic dykes, HP granulites, isothermal decompression, monazite geochronology.

1. Introduction

The Grenville Front is a NE-striking boundary (Fig. 1) SE of which Archean and Paleoproterozoic rocks of the Laurentian craton are reworked in the so-called Parautochthonous belt of the Grenville Province (Rivers et al., 1989). Within this belt, immediately to the southeast of the Grenville Front, rocks of Archean to Paleoproterozoic heritage that correlate with those of the Grenville foreland constitute a loosely defined zone of front-parallel fabrics known as the Grenville Front Tectonic Zone (GFTZ; Wynne-Edwards, 1972). This zone is affected by a short-lived, moderate temperature-high pressure metamorphic event at about 1 Ga, an event difficult to fully unravel, however, because of the polycyclic nature of the terranes involved and the potential diachrony in mineral crystallization (see Rivers et al., 1989; Indares and Martignole, 1989a). In eastern Ontario, it has been convincingly demonstrated that the Mesoproterozoic Sudbury dyke swarm is

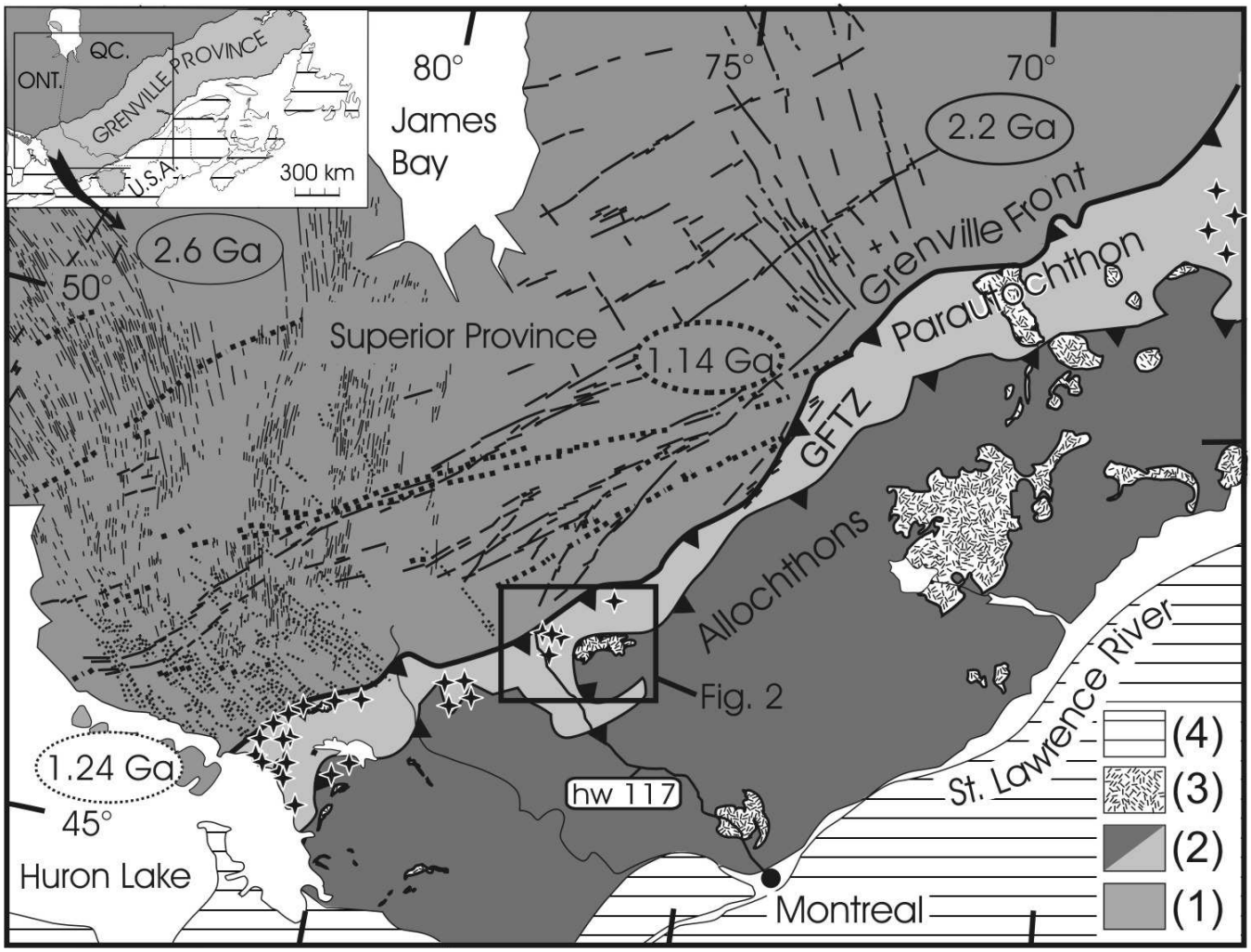

Fig. 1: Precambrian mafic dyke swarms of the Superior Province and reworked mafic rocks from the Grenville Front Tectonic Zone (GFTZ). Full thin and thick lines, dashed thin and thick lines correspond to different dyke suites respectively: Matachewan (2.6 Ga) and Preissac (2.2 Ga), Sudbury (1.24 Ga) and Abitibi (1.14 Ga), from Fahrig and West (1987) and Ketchum and Davidson (2000). Stars: high pressure rocks (Indares, 1993; Indares and Dunning, 1997; Ketchum and Davidson, 2000; present work). (1): Superior Province; (2): Grenville Province (Parautochthon and Allochthon); (3): Anorthosites; (4): Phanerozoic (Appalachian and Paleozoic cover).

intersected by the Grenville Front and is involved in intense Grenvillian deformation and metamorphism (Bethune, 1997; Bethune and Davidson, 1997). Several such swarms of Proterozoic mafic dykes intersect the Grenville foreland, and it is expected that their metamorphosed equivalents should be preserved SE of the Grenville Front. It is also likely that these dykes have registered the effects of the Grenville orogeny only. Their monocyclic nature would help characterizing the ubiquitous 1 Ga-old metamorphic event

typical of the GFTZ. The need for a better understanding of this zone becomes topical with the recent identification of another, less continuous belt that runs southeast of the GFTZ, namely the High-Pressure belt (Rivers et al., 2002). The aim of the present study is to use the metamorphosed equivalents of Proterozoic mafic dykes to monitor the ca. 1 Ga-old metamorphic event that characterizes the Grenville Front Tectonic Zone in western Quebec and to shed some new light on its metamorphic signature and tectonic significance.

2. Mafic dyke swarms of the Grenville foreland

Four major undeformed and unmetamorphosed dyke swarms crosscut the Archean rocks of the Superior Province and the Paleoproterozoic strata lying on top of the Archean craton (Southern Province, Mistassini and Otish basins), NW of the Grenville Front. They were all dated by U-Pb methods (Table 1). The oldest one is the Late Archean to Paleoproterozoic Matachewan swarm, followed by the Paleoproterozoic Preissac swarm, the remaining two being Mesoproterozoic, namely the Sudbury and the Abitibi swarms (Fig. 1). The Matachewan dykes, overlaid by Paleoproterozoic Huronian strata, strike N to NW and are about 10 m thick; they are quartz-tholeiitic and usually contain large calcic plagioclase megacrysts. Their U-Pb age is 2452 +3/-2 Ma (Heaman, 1989). They are limited to the western part of the Grenville foreland and do not seem to occur in western Quebec. The Preissac dykes, principally located in the Abitibi area where they strike NE, are subvertical and vary in thickness from a few metres to over 100 m; they are also quartz-tholeiitic and have been subdivided into an early group named Senneterre, dated at 2214 ± 12 Ma and a late group, named Biscotasing, dated at 2167 ± 1 Ma (Buchan et al., 1993). The Sudbury dykes are generally a few tens of metre thick and strike to the NW, orthogonal to the Grenville Front; they consist of olivine diabase with occasional plagioclase xenocrysts. They have a distinctive alkaline affinity (Ketchum and Davidson, 2000) and were dated at 1238 ± 4 Ma by Krogh et al.(1987. This swarm, like the Matachewan swarm, is essentially located in eastern Ontario but it is not excluded that

some units may occur in western Quebec. The Great Abitibi dyke (over 100 m thick and over 700 km long) is the most prominent unit of a NE-striking swarm, the Abitibi swarm which is dominated by olivine diabases and subordinate gabbros, diorites and monzodiorites (Ernst and Bell, 1992) with an alkaline chemistry; these rocks are younger (1140.6 ± 2 Ma; Krogh et al., 1987) than those of the Sudbury dykes. Since they are coeval with the Keweenawan rift magmatism and the Grenvillian orogenic cycle (1.2 Ga to 1.0 Ga), their emplacement has been considered as a side effect of the Grenville orogeny (Ernst et al., 1987).

Table 1: Summary of structural and geochronological data on mafic dyke –swarms, NW of the Grenville Front (see Fig. 1)

Dyke swarm		Strike	Thickness	Petrography	U-Pb Age
Abitibi		NE	Over? 100m	Olivine-gabbro	1141 Ma
Sudbury		NW	10-40m	Olivine-diabase	1238 Ma
Preissac	Biscotasing	NE	1-100m	Quartz-tholeiite	2167 Ma
	Senneterre				2214 Ma
Matachewan		N	~10m	Quartz-tholeiite	2452 Ma

3. Mafic dykes reworked in the GFTZ: Previous work

Mafic dykes and pods that are found SE of the Grenville Front, in the Parautochthonous belt of the Grenville Province, are likely to represent deformed and metamorphosed equivalents of the above mafic dykes. In Ontario, the Grenville Front intersects the Matachewan and Sudbury dykes at high angle. In western Quebec, the Front intersects the strike of Senneterre dykes at an angle of about 30º whereas the undifferenciated Preissac

and Abitibi dykes, striking NE like the Front, are only intersected in the vertical dimension (Fig. 2). The correlation between undeformed dykes and reworked equivalents is not everywhere obvious, although many of the mafic rocks of the GFTZ bear most of the chemical parameters of mafic dykes of the Grenville foreland. Moreover, these dykes having different structural settings and bulk compositions, various types of resulting strain patterns and mineral assemblages are expected in their Grenville Province metamorphosed counterparts. There is no precise age determination on metamorphosed mafic dykes in western Quebec, but most of these are either Paleoproterozoic Preissac dykes or Mesoproterozoic Abitibi dykes. Whether Sudbury dykes are represented needs to be demonstrated on geochronological bases. It should be noted however, that NW-striking dykes cross-cutting the Superior Province (eastern end of the Sudbury swarm; Fig.1) are probably present in western Quebec. Pending new geochronological determinations, discrimination between the various groups will be attempted on a geochemical basis. Several studies of the metamorphism that affected mafic rocks southeast of the Grenville Front have been carried in the last few years. In Ontario, rocks convincingly attributed to the Sudbury dyke swarm, on the basis of detailed mapping, geochemistry and geochronology (Bethune, 1997; Bethune and Davidson, 1997), were affected by Grenvillian (ca 1.0 Ga; Dudás et al., 1994) deformation at granulite-grade metamorphism (pressures up to 1 GPa). In western Quebec, gabbroic massifs intruded at 1217 +15/-10 Ma (potential equivalents of Sudbury dykes) underwent Grenvillian (1069 ± 3 Ma) granulite metamorphism, also at pressures of about 1 GPa (Indares and Dunning, 1997). Tectonic models accounting for the moderate to high-pressure metamorphism registered by these rocks essentially rest on crustal thickening via piling up of thrust slices (e.g. Bethune and Davidson, 1997). Finally, it should be noted that most of the rocks undoubtedly identified as reworked mafic dykes are located in the GFTZ and more widely in the parautochthon (Ketchum and Davidson, 2000), namely the footwall of major allochthons and thus structurally underneath the ``High-Pressure belt´´ of Rivers et al. (2002).

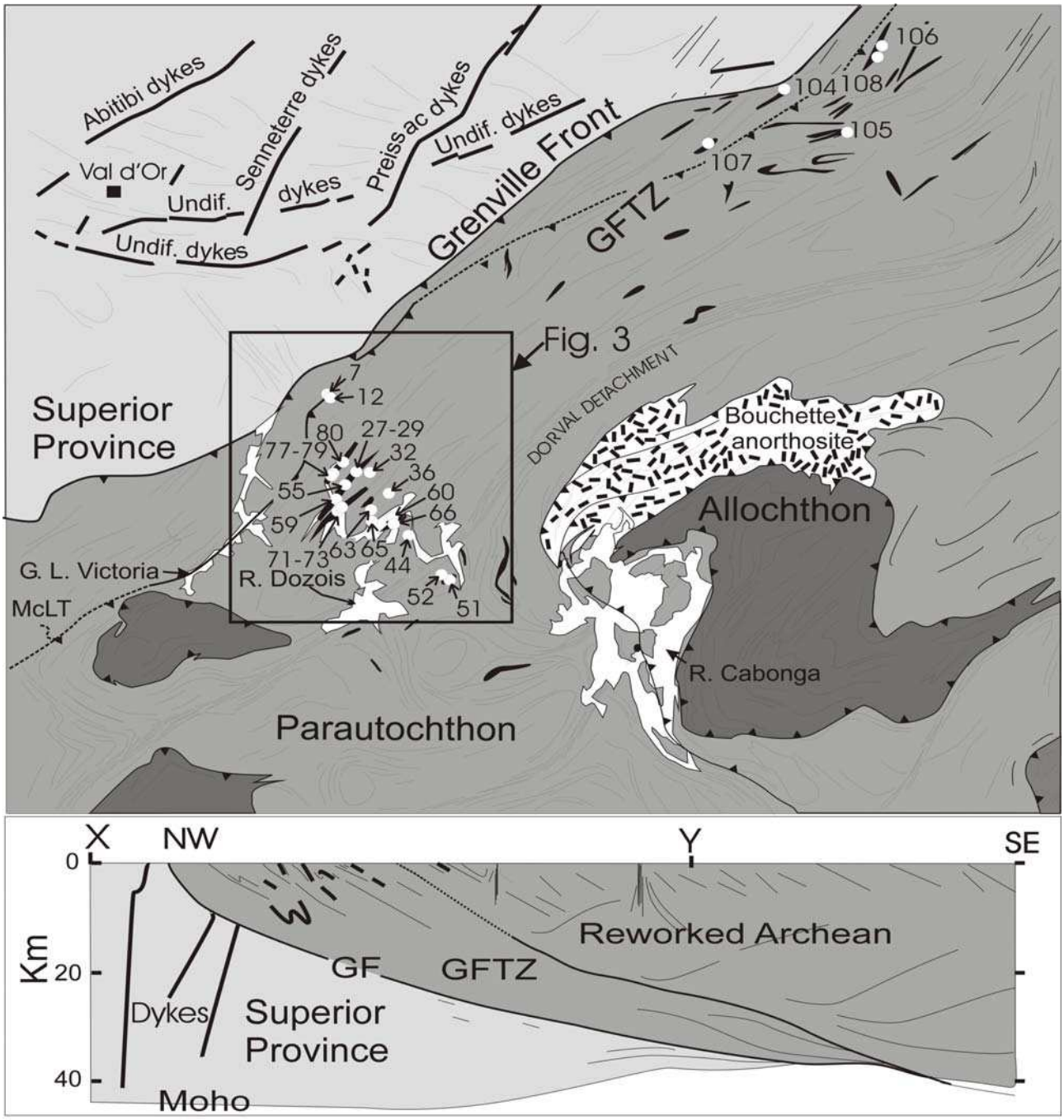

Fig. 2: a) The Grenville Front Tectonic Zone in western Quebec, with mafic dykes in black; location of samples referenced in text; tectonic map drawn from Avramtchev and LeBel-Drolet (1981) and Martignole and Pouget (1994); b) Vertical cross-section modified from Martignole et al., (2000).

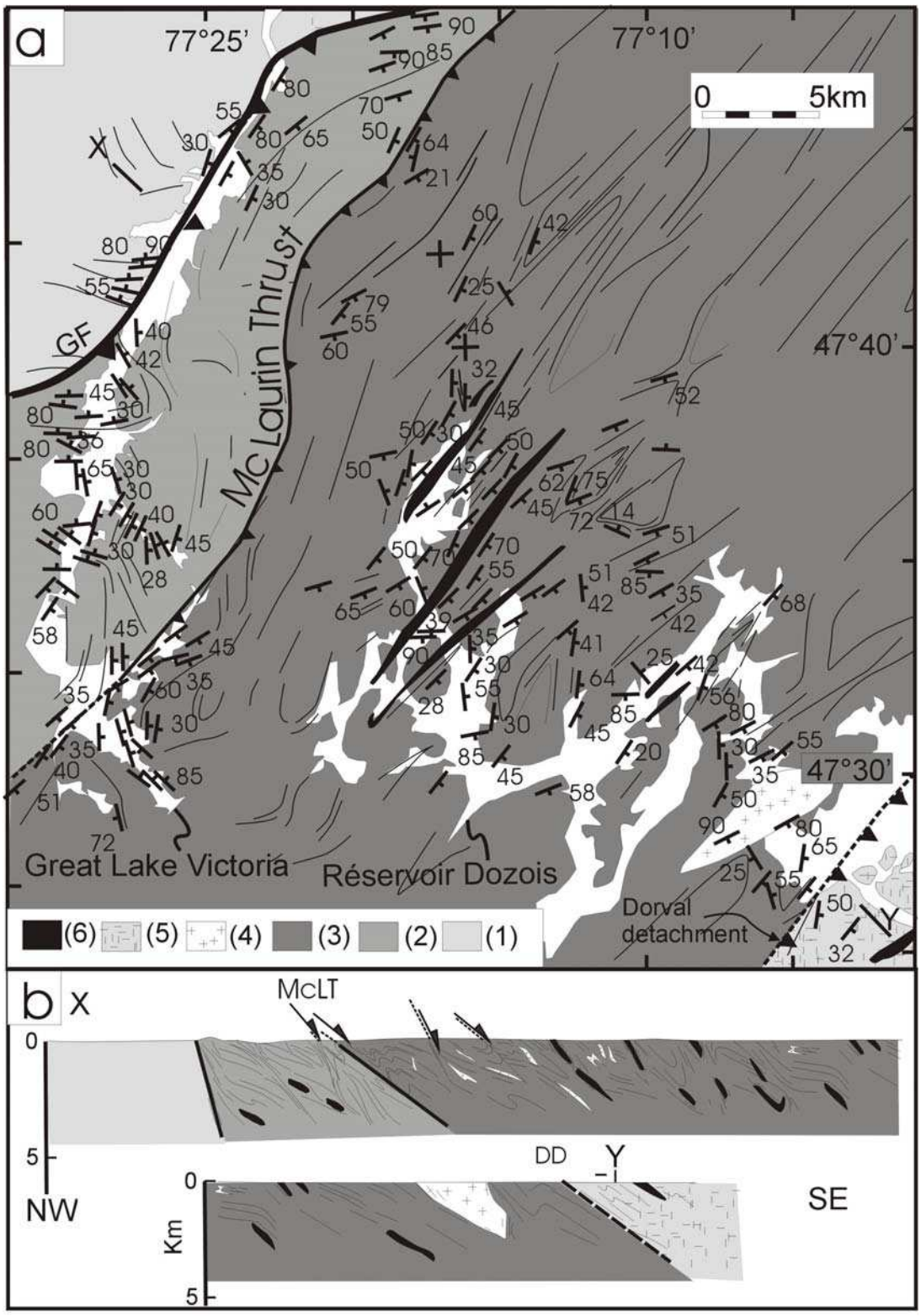

Fig. 3: a) Tectonic setting of mafic dykes; b) Cross-section through the GFTZ (1): Archean; (2): Pontiac schists; (3): migmatites and biotite or orthopyroxene-bearing gneisses; (4): biotite-(hornblende) migmatites; (5): Archean Dorval syenite; (6) mafic rocks.

Fig. 4: MacLaurin thrust : S-shaped fold in charnockitic gneisses overriding micaschists; late extensional shear zone affecting the inverted limb of the fold (Highway 117; 8 km SE of the Grenville Front).

4. Geological framework of the GFTZ in western Québec

A 60 km-long composite section of the GFTZ in western Quebec was achieved by combining information collected in the Forsythe area (Girard and Moorehead, 1994), along Highway 117 and also along the shoreline of Great Lake Victoria and Réservoir Dozois. Sm/Nd model ages (Dickin et al., 1989) show that the host rocks of the mafic dykes were generated by crustal extraction from the mantle at the end of the Archean. Mafic dykes and gabbroic masses have been mapped together with their medium- to high-grade host rocks southeast of the Grenville Front (Fig. 2, 3). Three main units can be identified SE of the Front, namely a unit made of medium-grained muscovite-sillimanite schists, with occasional kyanite (reworked Pontiac metasediments; Lac Témiskamingue Terrane of Indares and Martignole, 1989a; metamorphic conditions: P=450-550 MPa,T=590-670°C); a thick slab of orthopyroxene-bearing quartzofeldspathic rocks (second unit) overriding

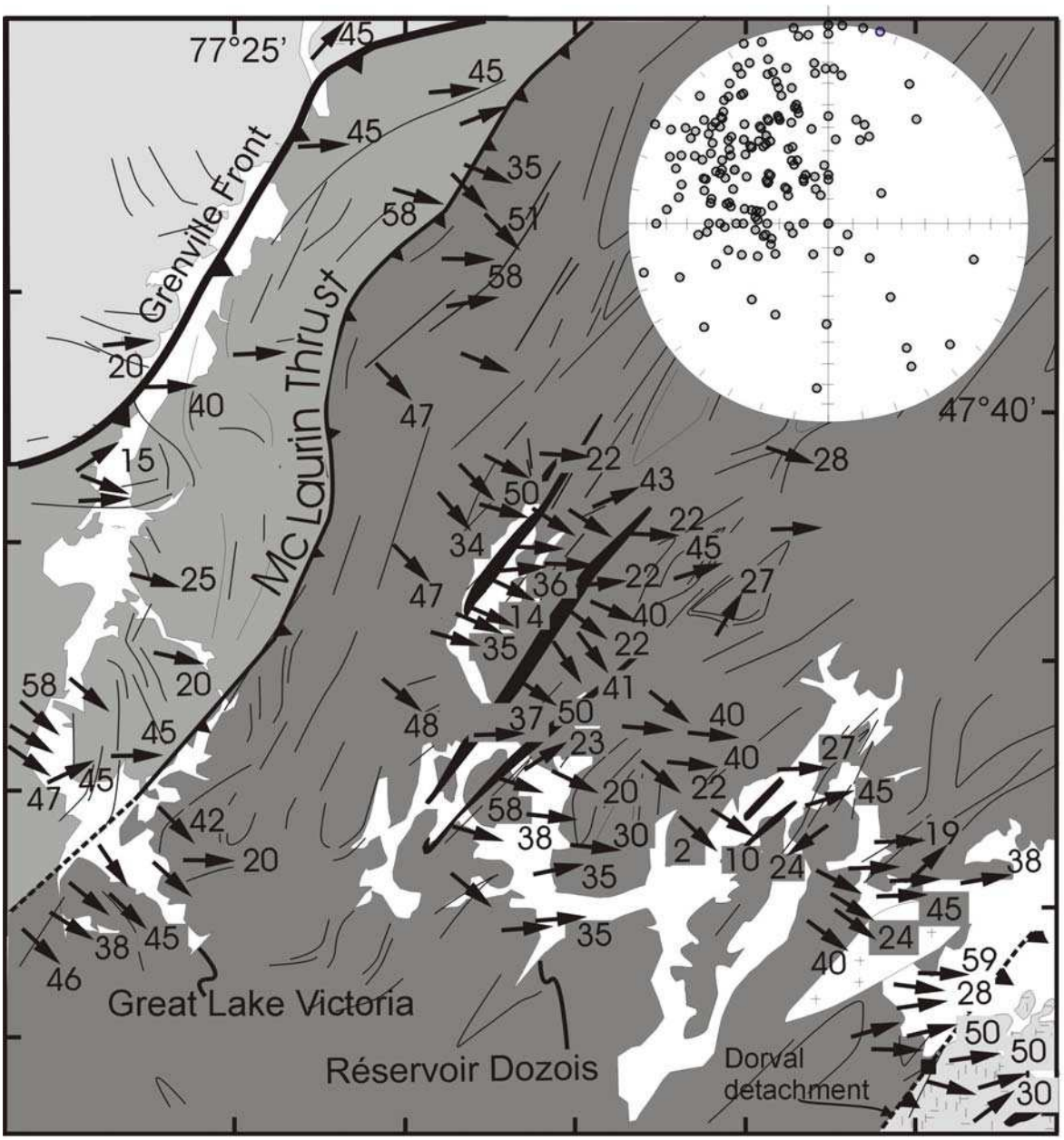

Fig. 5: Stretching and mineral lineations in the GFTZ and stereo-projection of foliation poles (lower hemisphere) for the same locations.

the schists along a metre-scale mylonite zone with top to the NW kinematic indicators, the McLaurin thrust (Fig. 3, 4, 5); above the McLaurin thrust, SE-dipping biotite-orthopyroxene-garnet gneisses and charnockitic gneisses, with SE-dipping stretching lineations (Fig. 5) constitute a ``granulite slab´´ (X Terrane; Indares and Martignole, 1989a; metamorphic conditions: P=790 MPa, T=720°C) that is the locus of NW-directed

thrust tectonics and SE-directed extension (Fig. 4; Indares and Martignole, 1989a and b). This granulite slab in turn dips southeastward under amphibolite-grade migmatites (the third unit) of the Réservoir Dozois terrane (metamorphic conditions: P=775 MPa, T= 690°; Indares and Martignole, 1990), probably along a SE-dipping extensional shear zone, the Dorval detachment (Fig. 2, 3). An anticlockwise rotation of the lineation trend is in keeping with sinistral extension along this detachment (Fig. 5) that is thus interpreted as transtensive shear zone.

5. Geochronological framework of the GFTZ

The geochronological framework of the GFTZ was elaborated during the last two decades using Rb-Sr methods (Doig, 1979), U-Pb methods (Philippe et al., 1990; Childe et al., 1993; Krogh, 1994; Martignole and Friedman, 1998), Pb-Pb method (Gariepy et al., 1990) and $^{40}Ar/^{39}Ar$ method (Martignole and Reynolds, 1997). U-Pb Archean ages of 2652 +9/-4 Ma were obtained on monazites from a quartzofeldspathic schist and a quartzofeldspathic gneiss from the footwall of the McLaurin thrust in addition to an age of 2665 +7/-6 Ma from a garnet-orthopyroxene gneiss located at 32 km south of the Front (Philippe et al., 1990). Lower intercepts of concordia for these samples point to Grenvillian lead loss at about 1 Ga. Concordant and oblique leucosomes from migmatites within the granulite slab contain monazites that also yielded Archean ages (Philippe et al., 1990). Zircon extracted from a metre-wide orthopyroxene-bearing pegmatite located at about 30 km south of the Front yielded an age of 2643 +/-5 Ma (Krogh, 1994). Finally, a SE-dipping gneissic pegmatite with top to the NW kinematic indicators yielded U-Pb ages of 2643 +6/-5 Ma on zircon and monazite (Martignole and Friedman, 1998).

Pb-Pb isochrons on quartzofeldspathic gneisses (reworked Pontiac schists), charnockitic gneisses (granulite slab) and pegmatites, also yielded Archean ages, whereas ca. 1 Ga-old ages were obtained on apatites that appear to be the only mineral reset with respect to lead isotopes (Gariépy et al., 1990). Above the granulite slab, in the hanging wall of the Dorval

detachment (50 km south of the Front), U-Pb data on monazites extracted from migmatites of Archean heritage (Dickin et al., 1999) yielded ages around 1.0 Ga, an evidence for complete Grenvillian recrystallization or isotopic resetting (Childe et al., 1993; Martignole et al., 2000). Finally, $^{40}Ar/^{39}Ar$ cooling ages on hornblende (Martignole and Reynolds, 1997) show that cooling through about 450ºC occurred at 995 ±12 Ma within the granulite slab, but was much later (around 960 Ma) in the migmatites of the hanging wall of the Dorval detachment. All the above data are in agreement with a high grade Archean isotopic signature around 2.7 Ga and a mild resetting around 1 Ga, hereafter referred to as Grenvillian.

In order to better constrain the sequence of metamorphic events in the GFTZ, we estimated Th-U-Pb chemical ages on monazite by *in situ* microprobe measurements using calibration and statistic treatment of Montel et al. (1996). Analyses were performed on a Cameca SX100 electron microprobe with four-wavelength dispersion spectrometer detectors at the 'Laboratoire Magmas et Volcans' (Clermont-Ferrand, France), according to the procedure described in Goncalves et al. (2003). An accelerating voltage of 15 kV and a beam current of 150 nA were adopted. U and Th were analyzed successively with a PET crystal in the same WDS detector with a counting time of 225 s and 75 s on peak, respectively. Pb was analyzed with a LPET crystal during 300 s on peak. Standards used are UO_2, ThO_2, vanadinite and a synthetic glass for Pb. Beam current used for standards is 100 nA. Counting time is 50 s on peak and 20 s on background for UO_2 and ThO_2, and 300 s on peak and 100 s on background for PbO. Individual ages were calculated using the decay scheme of Montel et al. (1996) from the Th, U and Pb concentrations assuming that all the lead in monazite is radiogenic in origin. The 2σ errors given on individual ages are calculated by propagating the uncertainties on U, Th, and Pb concentrations (with 95% confidence level). Calculation of mean ages and associated errors (95% confidence level) is based on least squares modeling, which discriminates multiple age populations. The quality of modeling can be assessed from the mean square weighted deviation (MSWD).

Th-U-Pb chemical ages were obtained on monazites from charnockitic gneisses (samples 7, 36; Fig. 2) and biotite-garnet gneisses (samples 12, 32, 44) from the GFTZ as well as from a garnet-sillimanite gneiss (sample 52) of the overlying Reservoir Dozois terrane. Monazite occurs either in the quartzofeldspathic matrix of these rocks or within the biotite, more rarely in garnet. The shape of monazite is highly variable from irregular stubby to elongated grains varying in size from 10 to 200 μm.

For sample 7, a strained charnockitic gneiss from the hanging wall of the McLaurin thrust, all analyzed monazites (including the smallest ones at 20 μm), yielded homogeneous Archean ages that vary between 2528 and 2848 Ma (50 measurements), with an acceptable statistical value of 2652 ± 28 Ma (n = 22, MSWD 0.52). At the same location, an orthopyroxene-free gneiss collected in a 10 m-wide SE-dipping extensional mylonite (sample 12), contains very fine-grained monazites (< 10 μm) from which eight crystals have been analyzed and yielded Grenvillian ages only, with a mean value of 987 ± 25 Ma (11 analyses).

For sample 32 (a coarse biotite-garnet gneiss; Highway 117; Fig. 2) 10 monazites were analyzed and yielded two individual ages at 1041 ± 60 Ma and 976 ± 60 Ma, whereas 26 analyses yielded ages ranging between 2340 Ma and 2823 Ma (with a statistical population at 2684 ± 34 Ma, MSWD 1.27). The oldest age (2823 Ma) is from a small (20 μm) rounded monazite included in a garnet megacryst, whereas the two Grenvillian ages correspond to monazites from a biotite-quartz symplectite. In sample 36 (a charnockitic gneiss), Grenvillian and Archean ages were obtained on a single monazite grain, whether it is from the matrix or the biotite. Two monazites included in garnet returned Archean ages only. Statistical ages for sample 36 result in two populations at 1006 ± 22 Ma (n = 9) and 2524 ± 25 Ma (n = 20). Sample 44, a biotite mylonite collected from a dark, SE-dipping, metre-scale extensional shear zone of the footwall of the Dorval detachment, contains elongated monazites rarely associated with zircon; a total of 34

measurements on 14 grains yielded ages between 948 and 1088 Ma, with a statistical age of 964 ± 28 Ma (MSWD 1.4). Finally, at about 4 km to the south of Dorval detachment (Reservoir Dozois terrane), 28 analyses were performed on 11 monazite grains from sample 52. Two mean age values were obtained at 1020 ± 17 Ma and 2827 ± 48 Ma respectively, the later being found in large zoned grains (Fig. 6) as well as in small rounded ones (< 20 μm). This sample is so far the south-easternmost one to yield an Archean age, since further to the southeast all analysed monazites yielded Grenvillian ages (Childe et al., 1993). In summary, monazites from charnockitic gneisses (sample 7), from coarse-grained garnet-biotite gneisses (sample 32), and from the core of garnet megacrysts have generally escaped Grenvillian resetting and exhibit Archean Th-U-Pb ages, whereas monazites from finely recrystallized or mylonitic biotite-garnet gneisses (samples 12 and 44) are of Grenvillian ages only. In the garnet-sillimanite gneiss (sample 52) located above the Dorval detachment, in the Reservoir Dozois terrane, both Archean and Grenvillian ages are recorded, in the core and the rim of single monazite grains respectively. According to this work, no ages were found between 1 Ga and 2.6 Ga, attesting to the absence of Paleo- and Mesoproterozoic metamorphic events in the GFTZ of western Quebec. In particular, no traces were found of the igneous and subsequent thermotectonic activity recorded in the Ontario section of the GFTZ (Davidson and van Breemen, 1994). The metamorphic imprint on all the Proterozoic mafic dykes is thus monocyclic and Grenvillian in age. Moreover, the Archean age of the protolith being well established, and the oldest ages being found in monazites included in garnet, it can be concluded that the GFTZ was affected by a granulite-grade metamorphic event around 2.7-2.8 Ga. Resetting around 1.0 Ga is pervasive in mylonitic zones of the GFTZ, but was not efficient enough to erase the Archean isotopic signature in less deformed rocks. As relatively high temperatures were attained during the 1.0 Ga metamorphic event, it is likely that the short duration of the Grenvillian event is responsible for the preservation of Archean ages. South of the Dorval detachment resetting of U-Pb systematic in monazites is pervasive (Childe et al., 1993).

Finally, the concentrations of ages around 1 Ga obtained by U-Pb, Th-U-Pb and hornblende $^{40}Ar/^{39}Ar$ methods is an evidence for rapid cooling of the GFTZ just after 1 Ga (Martignole and Reynolds, 1997).

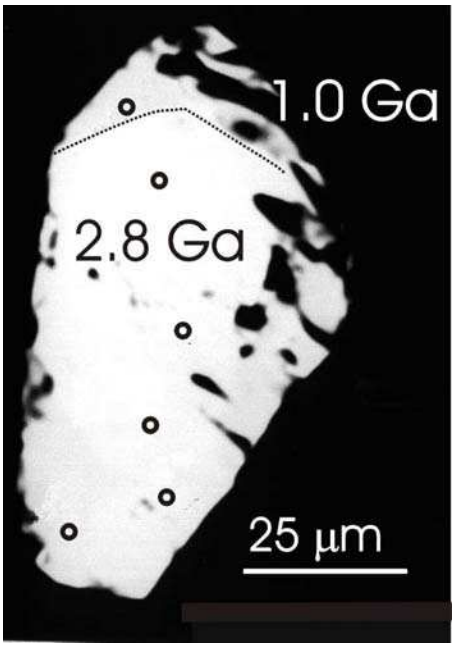

Fig. 6: Back-scattered image of a monazite grain from a biotite-garnet gneiss of the GFTZ showing analyzed points and calculated U-Pb-Th ages.

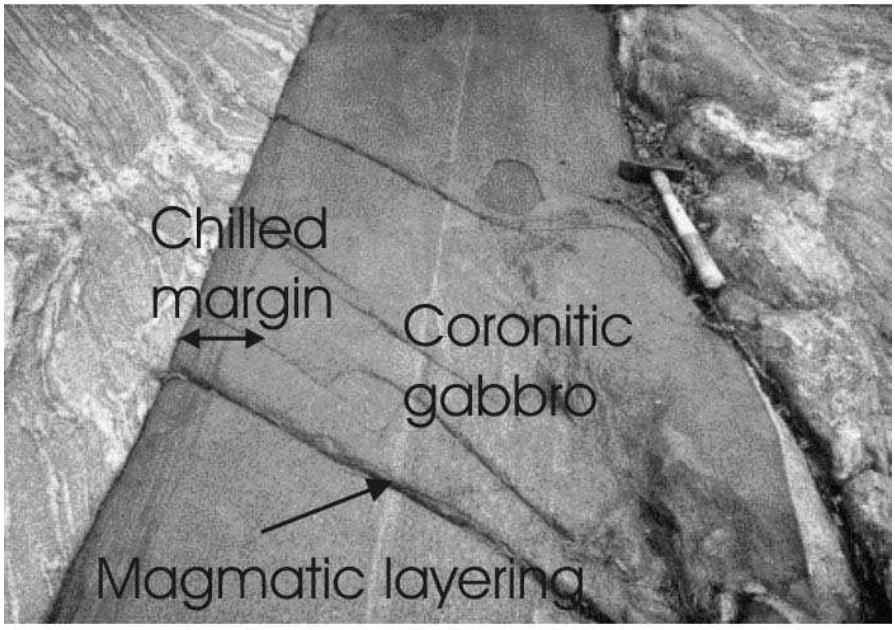

Fig. 7: Proterozoic (Abitibi or Sudbury) dyke of coronitic metagabbro cross-cutting gneissic Archean fabric and leucosomes.

6. Reworked mafic rocks: field occurrence

Mafic rocks of the GFTZ in western Quebec occur as metre- to decametre-scale, steeply dipping fine-grained dykes or as decametre-scale masses of medium- to coarse-grained coronitic leuco- to mesocratic gabbros. Although the contact between these mafic units and the surrounding gneisses is in many places mylonitic, metre-scale dykes are locally found to intersect regional foliation of biotite-garnet or charnockitic gneisses, in keeping with emplacement within high-grade rocks affected by fracturing in a brittle regime (Fig. 7). Also, chilled margins, a few centimetres in width, are compatible with intrusion at relatively shallow levels. Magmatic layering is common and usually sub-parallel to the margins of the metre-scale dykes, whereas in the central part of wider dykes, it is usually at angle with the contact. Centimetre-scale layering in the thickest dykes, is strongly reminiscent of the one found in layered igneous complexes and can locally be interpreted in terms of way-up criteria. In spite of the preservation of igneous characters, most of the mafic rocks within the dykes can be described as coronitic gabbros, with hornblende and garnet as the ubiquitous corona-forming minerals.

Intrusive contacts of medium- to coarse-grained leuco- to mesocratic gabbros are not exposed, and, given the restricted size of exposures, these rocks cannot be related to a specific type of structure. They may represent either the inner parts of thicker dykes or fragments of layered complexes that were dismembered during post-consolidation deformation. Alternatively, they may have intruded, deeper in the crust, as irregular masses under a more ductile regime.

The question thus arises as to the level of emplacement of mafic rocks in the GFTZ. Although deep-seated emplacement of dykes is debatable, both on mechanical and petrological grounds (e.g. Kuehner and Green, 1986), chilled margins and injection of fine-grained mafic rocks into brittle fractures are in keeping with emplacement of most dykes under hypabyssal conditions. In the GFTZ of eastern Ontario, the Sudbury dykes contain magmatic baddeleyite 250 m.y. older than ca. 1 Ga (Grenvillian) metamorphic zircon (see

Bethune & Davidson, 1997) developed during a late medium- pressure metamorphic event. Moreover, in this area, the Sudbury dykes intersect steeply dipping, 1.45 Ga-old NE-striking fabrics, attesting to a pre-Grenvillian exhumation of this section of the GFTZ (Bethune and Davidson, 1997). Similarly, in western Quebec, mafic dykes with chilled margins intersect gneissic and migmatitic foliation of Archean gneisses (Fig. 3 and 7), showing that not only significant late Archean unroofing had taken place SE of the Grenville Front but that the structural grain in the GFTZ was largely determined by these times. Cooling at depth thus seems to be excluded and late-formed minerals such as coronitic garnet or hornblende will be interpreted as metamorphic in origin.

7. Geochemistry

A series of whole rock analyses (major elements and selected trace elements) for the main mafic dykes and pods is presented in Table 2. Mafic rocks of the GFTZ of western Quebec can be subdivided into two compositional groups based on their silica content (silica-poor rocks with SiO_2<49% and silica-rich rocks with SiO_2>49%; see Table 2). This subdivision holds true in a (K_2O+Na_2O) vs SiO_2 diagram (Fig. 8a) and in the MgO vs K_2O, Fe_2O_3, Zr, and Ba diagrams (Fig. 8b):

a) a group plotting in the field of alkaline basalts (samples 51, 71, 72, 73, 79, 80, 105); this group is in fact comprised of low SiO_2 (~46%), high Fe_2O_3 total (~ 17.7%), high TiO_2 (~2.9%) rocks with low Mg-number (~40) and high Zr (~210 ppm).

b) a group corresponding to the compositional field of sub-alkaline or tholeiitic basalts (samples 28, 29, 55, 59, 63, 65, 104, 106, 107, 108) with SiO_2 >49%, moderate Fe_2O_{3total} (~10.5%), relatively low TiO_2 (~0.75%), average Mg-number (~55) and low Zr (~64 ppm).

The first group is best represented in the field by fine to medium-grained mesocratic dykes with well-preserved magmatic fabrics, whereas the second group comprises medium-grained, lighter coronitic gabbros. The bulk chemistry of the first group is reminiscent of that of the Sudbury dykes and to a lesser extent to that of the Abitibi dykes, both having

alkaline affinities. The Abitibi dykes, however, are less iron-rich and less Zr-rich whereas they are slightly richer in Ba. According to their chemistry (Fe, Zr and Ba contents), silica-poor dykes from the GFTZ are thus chemically more akin to those of the Sudbury swarm rather than to the Abitibi dykes (Fig. 8b).

The bulk chemistry of the second group is very close to that of the Senneterre diabase (Ernst, pers. comm. 2002) that belong to the Preissac swarm (Fig. 8a), with identical SiO_2 (~51%), total alkali ($Na_2O + K_2O$ ~ 3.2), average Mg-number (~0.55) and Zr (~ 64 ppm). Occurrences of mafic rocks in the GFTZ will thus be identified according to their belonging to one of the above groups.

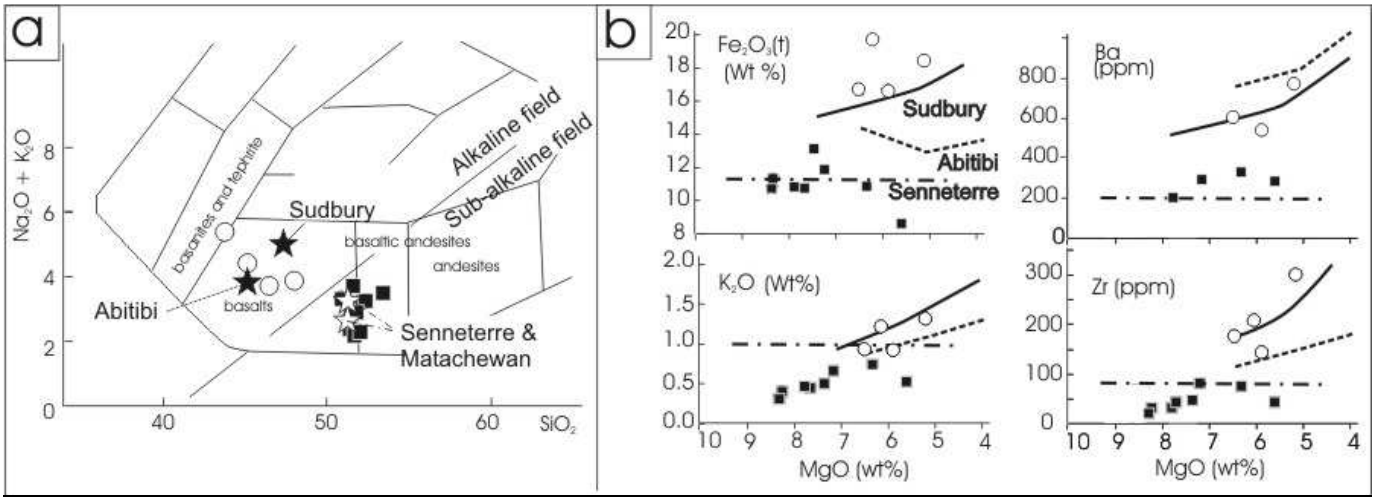

Fig. 8: (a) Chemical characteristics (major elements) of mafic dykes from the Superior Province and mafic rocks of the GFTZ; ■: dykes of sub-alkaline affinity (Senneterre and Metachewan swarms: white stars); ○: dykes of alkaline affinity (Sudbury and Abitibi swarms: black stars; Ernst, pers.com.; Buchan et al., 1993; Bethune and Davidson, 1997; Ernst and Bell, 1992). (b) Fe_{tot} (plotted as Fe_2O_3), K_2O, Zr and Ba versus MgO diagrams for mafic rocks of the GFTZ (full line and dashed lines: trend of Sudbury, Abitibi and Senneterre dykes, from Ketchum and Davidson, 2000).

8. Petrography of the mafic rocks

The texture and mineralogy of the mafic rocks vary with distance from the Front and with bulk chemical composition. As a general rule, well-preserved igneous (sub-ophitic) textures are common close to the Front, whereas fully granoblastic, metamorphic textures

are characteristic of the mafic inclusions within the migmatites of the Reservoir Dozois Terrane. The influence of global composition is also evident when considering the textural differences, silica-rich rocks being more affected by recrystallization and retrograde reactions than silica-poor rocks.

8.1. Silica-poor mafic rocks. (samples 51, 71, 72, 73, 77, 78, 79, 80, 105; see Fig. 2 for location of samples). Considering their bulk chemistry, these rocks could be described as high-Fe, titaniferous olivine-microgabbros and microdiorites. Although rocks of this group are garnet bearing, the coronitic texture is not as obvious as it is in the silica-rich metagabbros. Silica-poor gabbros are usually mesocratic; they have a trachytic texture defined by elongated cloudy plagioclase and interstitial clinopyroxene with schiller plates (Fig. 9). Plagioclase megacrysts (several mm) are occasional, as are olivine relicts, in the form of mm-scale serpentine clusters. Other magmatic minerals include brown hornblende, mm-scale apatite and Fe-Ti oxides that are usually surrounded by brownish-red biotite. Metamorphic minerals occur as coronas of green hornblende and/or garnet, with some occasional orthopyroxene. Blade-shaped garnet nucleates parallel to the albite twin of primary plagioclase. Metamorphic plagioclase is less abundant than primary plagioclase and is irregular in shape and free of inclusions. The likely presence of olivine on the liquidus precludes a deep-seated crystallization of the dykes. Consequently, garnet should be metamorphic, although its sub-solidus growth from plagioclase upon cooling at moderate pressure is not excluded.

8. 2. Silica-rich mafic rocks. (samples 27, 28, 29, 59, 60, 63, 65, 66, 104, 106, 107, 108). In the coronitic gabbros, igneous sub-ophitic textures with interstitial pyroxenes clouded by schiller inclusions are locally preserved. No trace of serpentine (that may attest to the former presence of olivine) has been observed, in agreement with the silica-saturated or oversaturated composition of the rocks. Metamorphic minerals generally occur as coronas around orthopyroxene and clinopyroxene. They are dominated by green hornblende and garnet, both minerals usually containing vermicular quartz. Garnet in turn may be replaced

by a symplectitic intergrowth of orthopyroxene and plagioclase. Most coronitic gabbros were probably characterized by the magmatic assemblage orthopyroxene-(clinopyroxene)-(±inverted pigeonite)-plagioclase-Fe-Ti oxides-(±brown hornblende)-(±quartz)-(±biotite).

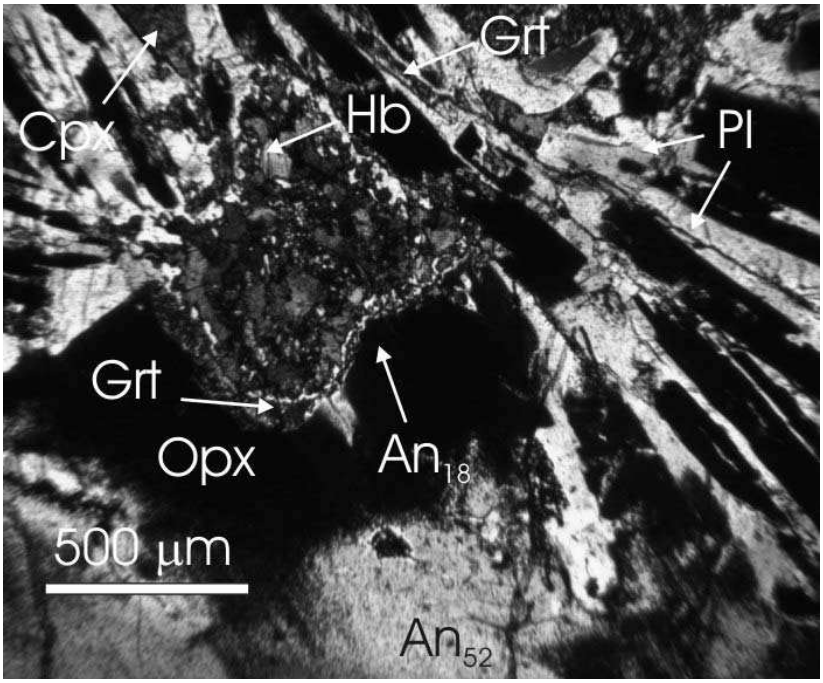

Fig. 9: Trachytic texture in the core of a silica-poor mafic dyke cross-cutting Archean gneisses of the GFTZ ; note the garnet blades within the plagioclase laths.

9. Mineral chemistry

Microprobe analyses of major phases are given in Table 3. Stoichiometric calculations were performed with the THEBA75 software (J. Martignole et al., unpub.) that estimates Fe^{3+} by charge balance.

9. 1. Orthopyroxene. Orthopyroxene is found as exsolutions in primary clinopyroxene, as megacrysts of igneous origin or as granoblastic (metamorphic) grains. Exsolved orthopyroxene is generally richer in Al_2O_3 and Cr_2O_3 than coexisting granoblastic orthopyroxene. Igneous orthopyroxenes are well preserved close to the Front. They are usually clouded with schiller inclusions and are rimed by either amphibole or garnet. They also tend to be richer in Al_2O_3 than the granoblastic ones. Most of the granoblastic orthopyroxenes are considered to be metamorphic in origin. In the silica-poor rocks,

metamorphic orthopyroxene usually occurs as small (< 20 μm) grains along the rims of clinopyroxene. This orthopyroxene (X_{Mg} = 0.47-0.64) is oxidized (Fe_2O_3 / Fe_{tot} up to 0.10) and has Al_2O_3 in the range 0.57 – 1.57 %. In the silica-rich rocks, X_{Mg} ranges from 0.56 to 0.69; Fe_2O_3 / Fe_{tot} is up to 0.16 and Al_2O_3 ranges from 1 to 2.13 %.

9. 2. Clinopyroxene. Most, if not all clinopyroxene megacrysts are considered to be magmatic in origin whereas smaller grains are considered as metamorphic. In the silica-poor rocks (samples 51, 79 and 80), clinopyroxene is diopsidic with X_{Di} in the range 0.60-0.70. Among the non-quadrilateral components, Al_2O_3 may be up to 4.84% and correlates with Na_2O higher than 2%. Accordingly, the jadeite content varies from 15 to 18 mol% in sample 80 and from 10 to 14 mol% in sample 79. Slight jadeite zoning is also noted (e.g. sample 51) from 7 mol% in the core to 4 mol% at the rim of the grain in contact with hornblende or plagioclase. There is thus a negative correlation between the jadeite content of the pyroxene and the SiO_2 content of the rock (Table 2). Ca-tschermak content, on the other hand, is very low and negatively correlated with Al_2O_3; it tends towards 0 in Na-rich pyroxenes, all the alumina being used up in the formation of the jadeite. In the silica-rich rocks, X_{Di} varies from 0.70 to 0.83 and the Al_2O_3 content ranges from 1.48 to 2.90%. The jadeite content is always lower than 4 mol%, and the Ca-tschermak content is lower than 0.029 mol%.

9. 3. Amphibole. Both green and brown amphiboles have been analyzed; they are calcic amphiboles (hornblende), having $Ca_B > 1.8$, $Na_B < 0.47$ and $(Ca + Na)_B > 2$. They plot along the limit between magmatic and metamorphic amphiboles in a Si/(Ca+Na+K) diagram (Fig. 10). In the silica-poor rocks, brown hornblende is considered to be magmatic whereas green hornblende such as the one found as coronas around orthopyroxene is considered to be metamorphic in origin. These hornblendes are low in silica (SiO_2 ranging from 38.1 to 44.96%); their Al_2O_3 content varies from 10.96 to 14.3%, with highest values found in brown hornblende. Na_2O varies from 3.25 to 1.31%, the highest values being from the brown hornblende. Finally, TiO_2 ranges from 3.7 to 1.8,

the brown hornblende being always above 2.3% TiO_2. In the hornblende from silica-rich rocks, SiO_2 ranges from 40.5% to 46.9%; Al_2O_3 from 10.5% to 15.0%; Na_2O from 1.1% to 1.6%; and TiO_2 ranges from 2.4% to 0.4 %. F and Cl are relatively low, although slightly higher than in the silica-poor rocks, especially concerning F.

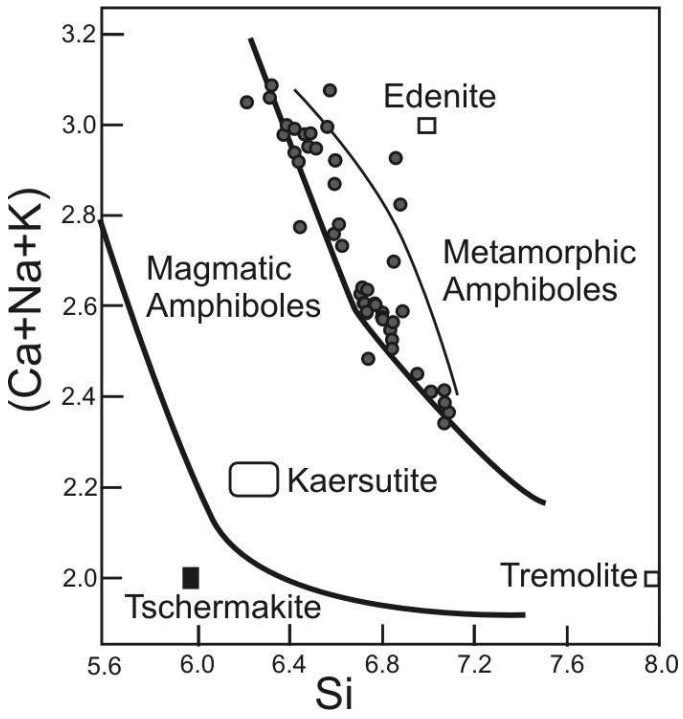

Fig. 10: Si *vs* Ca + Na + K diagram of amphiboles from the mafic dykes of the GFTZ

9. 4. Plagioclase. Both igneous and metamorphic plagioclases are present in most of the rocks analyzed although the distinction is not straightforward. In the silica-poor rocks, the anorthite content of clouded plagioclase megacrysts of likely magmatic origin is highly variable. In a first group of samples (e.g. sample 51), plagioclase exhibits a reverse type of zoning, with An_{25} in the core and An_{32} in the rim at the contact with garnet; small plagioclase grains are also in the An_{32} range. In a second group of samples (e.g. samples 71, 79 and 80) the core of megacrysts may be as high as An_{71} whereas the rims or the cores affected by secondary garnet growth may be as low as An_{11} (Fig. 9). In the silica-rich rocks with idiomorphic, non-corroded garnet (e.g. samples 55 and 28), plagioclase cores are at about An_{73} and the rims at An_{39}. In samples touching corroded garnet (samples 27, 60 and

66), cores are at An_{60} and inner rims at An_{47} whereas the outer rim may be as high as An_{83}. Associated, small, recrystallized plagioclase from finer grained symplectites is also at An_{83} (see Fig. 15). From textural considerations, it is clear that the increase in anorthite content of late plagioclase is related to the breakdown of the grossularite component of garnet. It should be noted, however, that in Si-poor rocks, the igneous fabric of the plagioclase may be preserved in spite of the involvement of this mineral in metamorphic reactions.

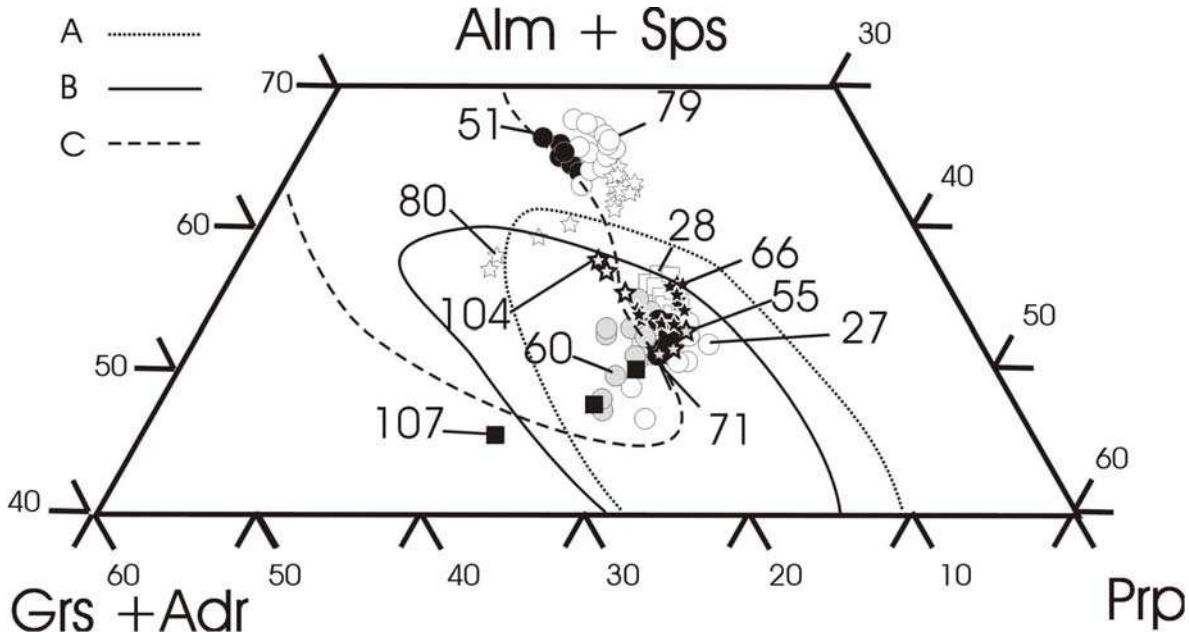

Fig. 11: Almandine + spessartine, pyrope, andradite + grossularite plot of garnet from the coronitic metagabbros (limits of compositional fields A, B and C for eclogitic garnets (after Mottana, 1984) drawn for reference (abbreviations according to Kretz, 1983).

9. 5. Garnet. Garnet, in virtually all the samples analyzed, is undoubtedly metamorphic in origin. Garnet analyses are plotted in the triangle (Alm+Sps)-Prp-(Grs+Adr) (Fig. 11) where they occupy the fields of eclogite garnets as delineated by Mottana (1986). Most garnets are symplectitic or coronitic phases; they are generally unzoned although their composition and size are strongly controlled by the nature of adjacent phases. Amphibolite grade garnets from the immediate vicinity of the Front (samples 107 and 104; Forsythe

area) are Ca-rich, with values in the ranges of Grs_{30-17} Adr_{3-2} Alm_{54-44} Sps_{3-1} $Prp_{28-22.}$ Garnets from the granulite slab plot in two domains of the garnet triangle (Fig. 11): Fe-rich garnets are characteristic of all but one of the silica-poor samples, while Mg-rich garnets are mainly found in the silica-rich samples. However, the grossularite content (commonly around 20%) is independent of this subdivision. Garnet with the highest Grs content (Grs_{25}; sample 80) is found in the silica-poor rocks. The relatively high Alm content in this garnet (up to Alm_{54}) is correlated with the high Fe content in the global composition (see Table 2). In general, in the silica-poor, Fe-rich rocks, the almandine content is thus largely controlled by the global composition. In the silica-rich rocks, the Grs content vary from Grs_{21} to $Grs_{15,}$ particularly where garnet is in contact with plagioclase, itself enriched in anorthite along its margins (e.g. samples 27, 60 and 66).

9. 6. Biotite. Biotite is common in some of the silica-poor rocks. Biotite in these rocks has intermediate Fe/Mg ratios (X_{Mg} =0. 44-0.41), from 14 to 15% Al_2O_3, relatively high titanium (TiO_2 = 3.15-3.87 wt%) and moderate amounts of ts-substitution (Al^{IV} around 0.1 on a 4 tetrahedral cations basis).

10. Phase equilibria

Starting from the ubiquitous magmatic assemblage plagioclase-clino (and/or ortho) pyroxene, the development of metamorphic minerals in mafic rocks of the GFTZ can be described using a limited set of components: SiO_2-Al_2O_3-CaO-FeO-MgO-Na_2O and H_2O (CFMANSH) meant to represent the ubiquitous phases: plagioclase, orthopyroxene, clinopyroxene, hornblende and garnet, with possible addition of quartz and olivine. Accessory phases like biotite, ilmenite and magnetite are linked to secondary components (K_2O, TiO_2, O_2) and can thus be considered as relevant to independent systems. Graphical analysis of mineral assemblages being limited to three or four components, it can only provide a partial representation of potential phases, in a system with a high number of components. Regrouping components like FeO and MgO or neglecting the albite

component in plagioclase allows the use of *ad hoc* representations like ACF diagrams. In natural assemblages however, large variations in FeO/MgO and Ab/An ratios increase the variance of the system hampering simple graphical analysis. Finally, it should be remembered that the pyroxene-plagioclase assemblage of the protolith is stable in low to intermediate pressure granulite facies. Textural analysis in many cases gives information on the way a bi- or trivalent assemblage is replaced by another one, thus providing an insight on the P-T path followed by the mafic rocks. Given these constraints, the growth and breakdown of major phases can be discussed starting from the Grenville Front.

10. 1. Phase changes in silica-rich rocks

10. 1. 1. Hornblende growth. In the Forsythe area, between 1 and 2 km from the Front (samples 104, 108; Fig. 2), mafic rocks have preserved their primary ophitic texture with slightly bent, zoned and cloudy plagioclase crystals and interstitial magmatic orthopyroxene. Coronas of bluish-green hornblende grew along orthopyroxene-plagioclase boundaries, with pure hornblende on the plagioclase side and hornblende-quartz symplectites on the pyroxene side (Fig. 12 and 13). Within the pyroxene surrounded by coronas, patches of retrogressive hornblende (Fig.13) suggest the former presence of plagioclase inclusions or the percolation of water that allowed the transport of alkalis and calcium. Brownish-green hornblende that grew at the contact between plagioclase and Fe-Ti oxides, was probably formed during a late magmatic stage when water activity was increasing in residual liquids and is thus not considered to be metamorphic. The growth of hornblende coronas and patches can be envisaged according to an amphibolite-grade model reaction:

(1) magmatic pyroxene + magmatic plagioclase + H_2O = metamorphic hornblende + quartz.

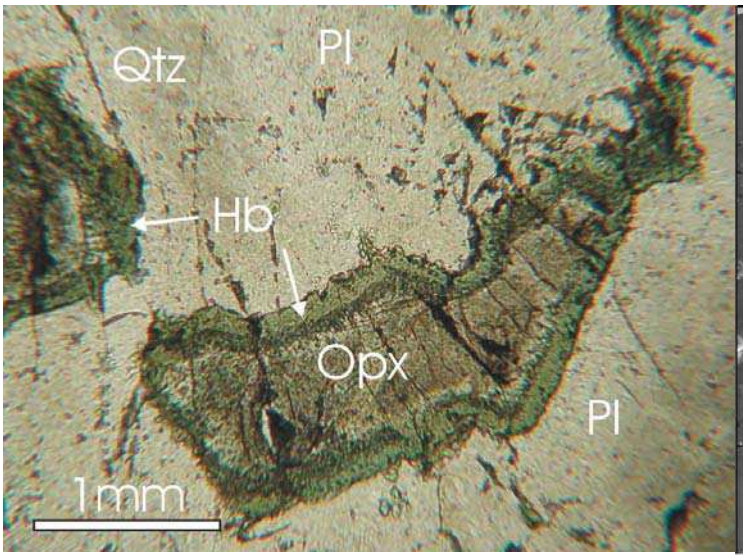

Fig. 12: Hornblende corona around magmatic orthopyroxene

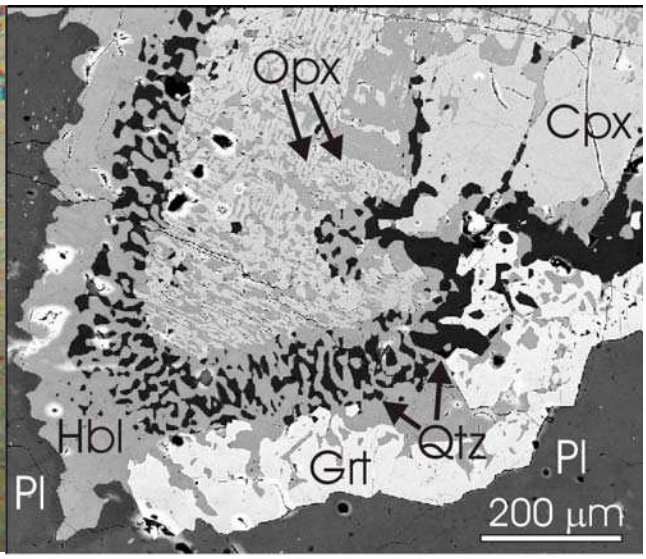

Fig. 13: Back-scatter image of hornblende-quartz(-garnet) symplectites around primary (magmatic) orthopyroxene (with hornblende-quartz symplectite on the pyroxene side), and hornblende replacement patches in the core of the orthopyroxene.

Hornblende being an interior phase in an ACF diagram, clinopyroxene as well as orthopyroxene may be involved in the reaction. Garnet is frequently associated with hornblende in the coronas (Fig 13), attesting to the metamorphic origin of the assemblage. Compared to the igneous assemblages, reaction (1) represents lower temperature conditions, higher water activity and probably higher pressure. Concerning the influx of water, textural evidence suggests that H_2O entering the hornblende structure is not coming from the breakdown of chlorite or epidote from a lower grade assemblage, both minerals being absent from these rocks. The general reaction:

(2) anorthite (in plagioclase) + H_2O = zoisite (in epidote) + quartz,

probably did not occur, although epidote is stable at relatively high pressure in the amphibolite facies. Hydration rather occurred, through fracture-controlled percolation or from infiltration of water released by prograde breakdown of hydrous phases (muscovite, biotite and staurolite) from the surrounding schists. The preservation of the initial

chemistry in the metamorphosed mafic rocks and the limited amount of hornblende produced being against large-scale water percolation, the second scenario is more likely. Moreover, the absence of chlorite and epidote in the mafic assemblages located immediately to the south of the Front, suggests overstepping or telescoping of the isograds. Reaction (1) thus occurred through hydration and heating up of the cooled down, dry magmatic pyroxene-plagioclase assemblages, above the stability field of both chlorite (T> 550°C) and probably epidote (T>670°C; e.g. Spear, 1993). The formation of hornblende outside the stability field of epidote, in the sillimanite stability field, but close to the kyanite-sillimanite inversion curve means that pressure was in the vicinity of 1 GPa.

At about 7 km from the Front (sample 107; hanging wall of the McLaurin thrust), the ophitic texture is largely destroyed by thorough recrystallization of plagioclase and to a lesser extent of pyroxenes. The few plagioclase megacrysts that escaped recrystallization are strongly bent and show undulatory extinction. Hornblende does not occur anymore as coronas but as isolated brownish grains developed on the pyroxenes. The modal proportion of hornblende is much less than near the Front. In this area, mafic rocks are embedded in charnockitic gneisses and quartzofeldspathic migmatites. The lower modal amounts of hornblende in the metagabbros may reflect the dehydrated nature of the surrounding rocks and limited amount of free water that was preferentially incorporated into silicic melts of the migmatites during peak metamorphism.

10. 1. 2. Garnet-forming reactions. In the immediate vicinity of the Grenville Front, garnet usually occurs, together with hornblende, as partial coronas between primary orthopyroxene and plagioclase. Garnet nucleated preferentially at the contact with plagioclase whereas the hornblende-quartz symplectite grew at the contact with the pyroxene (Fig. 13). As plagioclase coexists with hornblende, garnet formation cannot be due to a hornblende-plagioclase reaction. This garnet is thus generated during hydration of the rock according to an amphibolite grade model reaction of the type:

(3) orthopyroxene + plagioclase + H_2O = garnet + hornblende + quartz.

This reaction is coupled with the hydration of the orthopyroxene core that is locally converted into a hornblende-quartz symplectite.

Away from the Front, above the McLaurin thrust, orthopyroxene is stable in the host rocks of the dykes and hydration of the Opx-Pl assemblage is not pervasive, probably because host rocks were already dehydrated at the onset of the Grenvillian metamorphism. Garnet rather formed as corona along the contact between primary plagioclase and orthopyroxene or grew as an idiomorphic phase unrelated to corona textures. In this case, garnet is not anymore related to a hornblende-forming reaction, as above, neither it is the product of a hornblende + quartz reaction as usually observed in iron-rich rocks from the amphibolite-granulite transition. It was formed according to a solid-solid reaction of the type:

(4) orthopyroxene + plagioclase = garnet + quartz (±clinopyroxene),

a reaction with a large negative volume change compatible with metamorphism in the high-pressure granulite field. This reaction, responsible for the formation of the majority of coronitic textures in the metagabbros (Fig. 14), resulted in the reduction of the modal proportion of primary orthopyroxene in the southern part of the GFTZ at the pressure peak of metamorphism in this area.

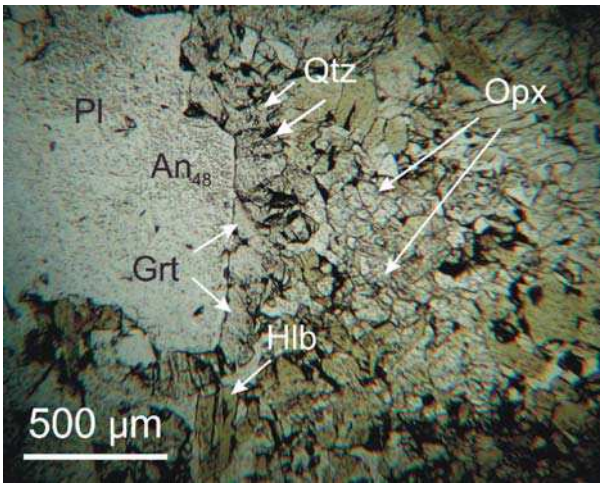

Fig 14: HP Granulite-grade garnet quartz corona

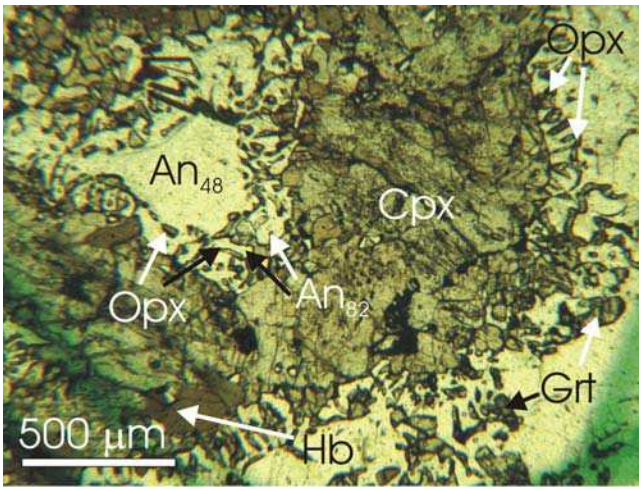

Fig. 15: Orthopyroxene-plagioclase symplectites, pseudomorphs of a former garnet-quartz corona (sample 66)

10. 1. 3. Garnet-consuming reaction. Starting at about 18 km from the Front, garnet coronas that formed according to reaction (4) are replaced by a plagioclase-orthopyroxene symplectite (sample 66; Fig. 15), resulting in a secondary (metamorphic) Opx-Pl assemblage. This texture probably stems from a back-reaction between garnet and quartz (reaction 4 in opposite sense) as attested by the local occurrence of corroded garnet, a leftover after exhaustion of quartz. This reaction has a gentle positive slope in a P-T diagram and is accompanied by a large volume increase, and as grain size of symplectitic minerals is much smaller than that of the initial garnet, it cannot record a long lasting high-T recrystallization regime. Isothermal decompression is thus the most likely scenario to account for these textures whose preservation is favoured by the dryness of the assemblage and probably by a rapid (isobaric?) cooling following the decompression stage. A portion of the P-T path, valid for the inner part of the GFTZ, thus includes a major isothermal decompression from the high-pressure granulite field into the intermediate to low-pressure field, probably followed by rapid cooling before returning to the actual level of exposure.

10. 2. Phase changes in silica-poor rocks

Besides the greater abundance in primary brown (titaniferous) hornblende, silica-poor rocks are characterized by the epitaxial growth of garnet within the plagioclase and the preservation of a high jadeite content in the clinopyroxene. Grossularite-rich garnet probably nucleated directly in the anorthite-rich core of igneous plagioclase under high-pressure conditions, according to the anorthite breakdown reaction:

(5) anorthite = grossular + kyanite + quartz,

while minor oxide inclusions in the plagioclase reacted with potential kyanite to form the almandine (sample 80; see Fig. 9). The high jadeite concentration is also evidence for the high pressure attained by these rocks, and the absence of back reaction to albite can be related to the low silica activity.

10. 3. Absence of melting reactions

None of the dykes or the coronitic gabbros presents evidence for secondary melting, even in the area of granulite-grade assemblages. As dehydration of hornblende is the main melt-producing reaction in dry mafic rocks, it is reasonable to consider that either hornblende did not form in these rocks during the prograde path or that, if it did form, the temperature required for fluid-absent melting of hornblende was not attained. Of course, around 800°C, the amount of melt produced by hornblende melting is probably very low in the absence of free water (e.g. Rushmer, 1991). If water is added, then melting is more likely to occur under 800°C (Springer and Seck, 1997). Water influx into the dykes at the peak of metamorphism is however unlikely, because it was hardly present as a phase at that stage. All the assemblages described above can thus be considered as sub-solidus.

11. Metamorphic conditions

There are some difficulties in assessing Grenvillian metamorphic conditions in host rocks (biotite-garnet-orthopyroxene gneisses, charnockitic gneisses) from standard geothermobarometric techniques because many high-grade metamorphic minerals are inherited from pre-Grenvillian (Archean) times (Indares and Martignole, 1989a, b) and also because high temperature and the presence of a melt phase at peak conditions have favoured element readjustments upon cooling. Therefore, the reconstruction of a reliable Grenvillian P-T path can only be based on the study of Proterozoic mafic rocks. Mineral assemblages, textures and mineral compositions in the mafic dykes provide the following clues for the metamorphic conditions during the Grenvillian event:

1) Between the Grenville Front and the McLaurin thrust, epidote is absent from the mafic rocks and kyanite (together with sillimanite) is occasionally found in associated aluminous rocks: P-T conditions were thus close to or above the intersection of the epidote-out curve with the kyanite-sillimanite inversion curve (about 1.0 GPa at 700°C; e.g. Spear, 1993);

2) In the same area, availability of free water allowed the formation of hornblende-quartz symplectites after magmatic orthopyroxene-plagioclase assemblages, during an amphibolite grade event. As free water was likely available, the absence of partial melting in mafic assemblages sets a maximum for the temperature at about 800°C;
3) In the granulite slab (above McLaurin thrust), hornblende is less abundant, the formation of garnet (probably through a plagioclase-orthopyroxene reaction) culminated during a high-pressure granulite stage and lasted until consumption (or shielding) of orthopyroxene; mafic rocks were probably dry without significant water influx from host rocks and partial melting is not observed where hornblende is present; all assemblages are thus sub-solidus, which means that the temperature cannot be much higher than 800°C in the case of silica-rich mafic rocks and a few tens of degrees higher for silica poor rocks under dry conditions (e.g. Rushmer, 1991). In some silica-undersaturated rocks, nucleation of garnet within calcic plagioclase attests to an incipient instability of plagioclase indicative of eclogite facies conditions. Eclogite-facies conditions are also recorded in the same rocks by the jadeite contents of the clinopyroxene (in excess of 10%), the omphacitic character being locally preserved thanks to the absence of free silica to promote the destabilization of jadeite.
4) This high-pressure stage was followed by back-reactions that gave rise to Opx-Pl fine-grained symplectites implying decompression and quenching of the textures probably due to rapid (isobaric?) cooling at moderate pressure. Rapid exhumation and cooling probably favoured the preservation of close to peak metamorphic compositions in most minerals. Finally, the absence of decompression melting implies that unroofing is accompanied by some temperature decrease in order to avoid intersecting the steeply positive melting curves of mafic compositions.

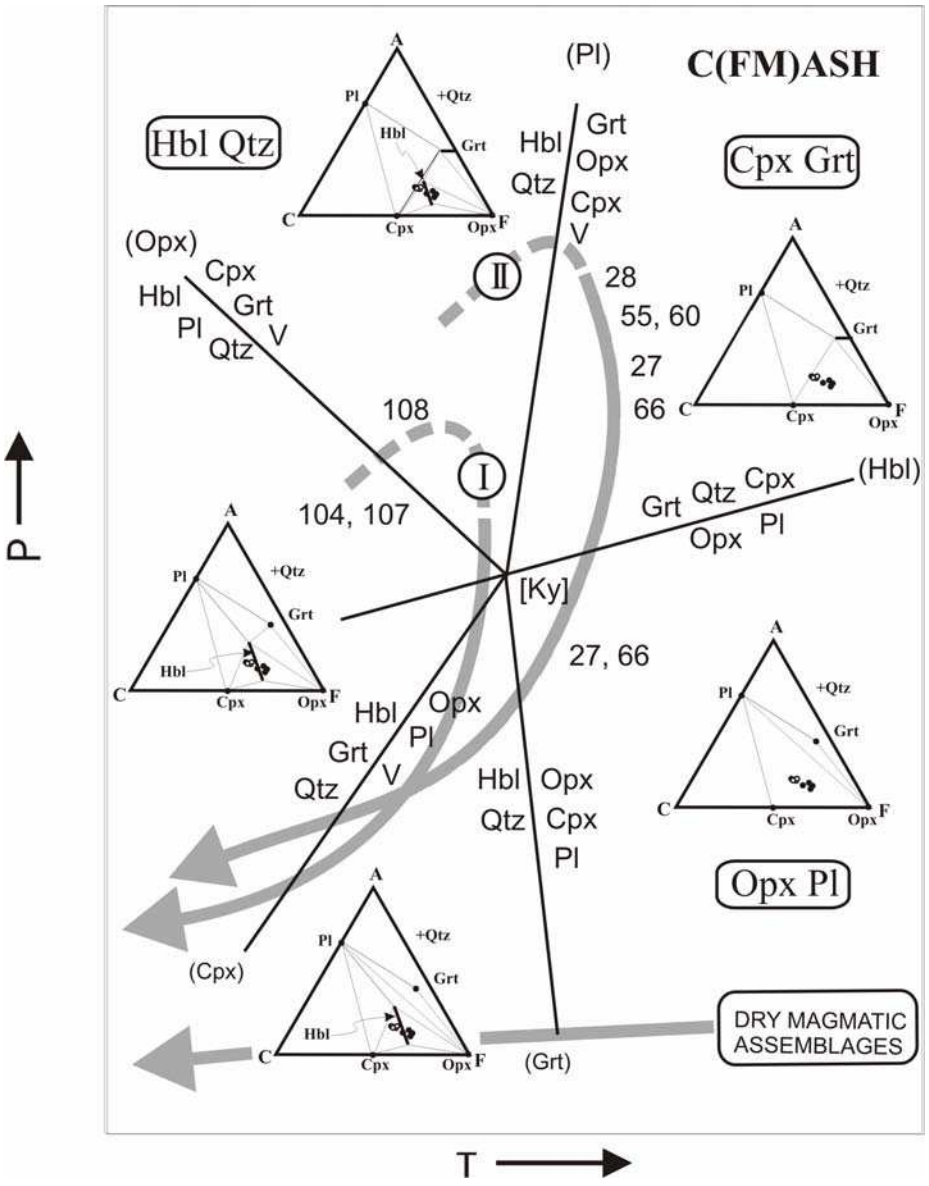

Fig. 16: Semi-quantitative P-T grid (CFMASH system) with interpreted paths for amphibolite grade rocks of the footwall of McLaurin thrust (I) and granulite grade rocks of the hanging wall of the McLaurin thrust (II); 28, 51, 60, 27, 66, 108, 107, 104: sample numbers.

The above reactions and the corresponding fragments of P-T path can be portrayed in a schematic petrogenetic grid in the C(FM)ASH system (Fig. 16), assuming excess silica, fixed plagioclase composition and Mg/Fe + Mg (Mukhopadhyay and Bose, 1994; Pattison, 2003). The immediate vicinity of the Front shows typical assemblages of the upper amphibolite facies (samples 104, 107 and 108) whereas the granulite slab experienced high-pressure granulite facies followed by isothermal decompression into the medium pressure granulite facies and finally by more or less isobaric cooling.

12. Geothermobarometry

As quantitative evaluation of intensive parameters in rocks that display evidence of disequilibria may be hazardous, care was taken to select micro-domains containing all the phases defining a given reaction with unzoned or slightly zoned minerals having regular contours and non extreme chemical compositions. Starting from these criteria, pressures and temperatures were calculated using THEBA75 software for solid-solid reactions (Martignole et al., unpublished) except for reactions involving hornblende for which the calibration and activity models of Mader and Berman (1992) and Mader et al. (1994) were adopted through TWQ (version 1.02, Berman, 1991). All the calculations were performed with the thermodynamic database of Berman (1988). End-member activities for garnet, pyroxenes and plagioclase were based on mixing on X, M1-M2 and T-T1 sites respectively. Deviation from ideal mixing was accounted for by excess energy parameters of Berman et al. (1995), Berman and Aranovich (1996), and Fuhrmann and Lindsley (1988) for pyroxene, garnet, and plagioclase. Estimations of temperatures are based on exchange reactions involving garnet and ortho- or clinopyroxene:

(6) En + Alm = Fs + Prp and

(7) Di + Alm = He + Prp

Resulting temperatures are considered as minimum estimates, due to possible Fe-Mg diffusion upon cooling. Pressures are derived from the garnet-forming reactions after plagioclase and orthopyroxene (Reaction 4), and plagioclase and clinopyroxene:

(8) Di + Pl = Grs + Prp + Qtz.

These reactions having gently positive slopes in a P-T diagram, readjustment of Fe/Mg ratios upon cooling will result in pressure estimates lower than peak pressures.

12.1. P-T Conditions close to the Grenville Front

Immediately to the SE of the Grenville Front (samples 104,107) temperatures were obtained using the calibration of Fe-Mg exchange between garnet and pargasitic

hornblende, whereas pressure was estimated from reactions between tremolite and plagioclase to produce garnet and tschermakitic-pargasitic hornbende:

(9) Tr + An = Ts + Prp+ Grs + Qtz and

(10) Tr + An +Ab = Pa + Prp+ Grs + Qtz

The magnesian pole of both reactions (equilibrium 3 and 5 of Mader et al., 1994) is considered to yield more reliable results. Starting from temperatures estimated with the Fe-Mg exchange (700-725°C), pressures were estimated to lie between 890 MPa and 950 MPa.

12. 2. P-T conditions above the McLaurin thrust

Temperatures determined from the Cpx-Grt exchange reaction vary from 730ºC to 828ºC (Table 4). Considering the possibility of Fe-Mg diffusion during cooling, it is likely that the upper values are more representative of the average temperature in the granulite slab at the thermal peak of metamorphism. Some temperatures below 700ºC are obtained with the Opx-Grt thermometer that may be more easily reajusted during cooling. If a temperature of 800ºC is adopted as a close to peak estimate, peak pressures calculated with the Pl-Cpx-Grt-Qtz assemblage (Reaction 4), vary between 1100 and 1400 MPa. The highest pressure is registered by a silica-poor rock (sample 80) that also has the highest jadeite content in the clinopyroxene (X_{Jd}>0.1), whereas the lowest pressure is from a silica-rich rock (sample 60), with a jadeite-poor clinopyroxene (X_{Jd}=0.03). It should also be noted that samples that have registered the lowest temperatures and the lowest pressures (samples 27, 60 and 66) are those where the garnet breakdown retrograde reactions have proceeded to near completion, probably because of the availability of quartz at the peak of metamorphism. It is thus possible that even the Pl-Cpx-Grt-Qtz assemblages underwent post-peak compositional readjustment, resulting in lower pressure estimations.

12. 3. Retrograde conditions

Retrograde conditions are provided by the breakdown of garnet in silica-oversaturated mafic assemblages and the formation of Opx-Pl symplectites. Orthopyroxene-garnet

exchange thermometry applied to these symplectites combined with barometric calibration of the Grt + Qtz = Opx + Pl reaction (Reaction 4; Table 4) yield conditions between 733ºC and 682ºC, with pressures of 825 MPa to 975 MPa.

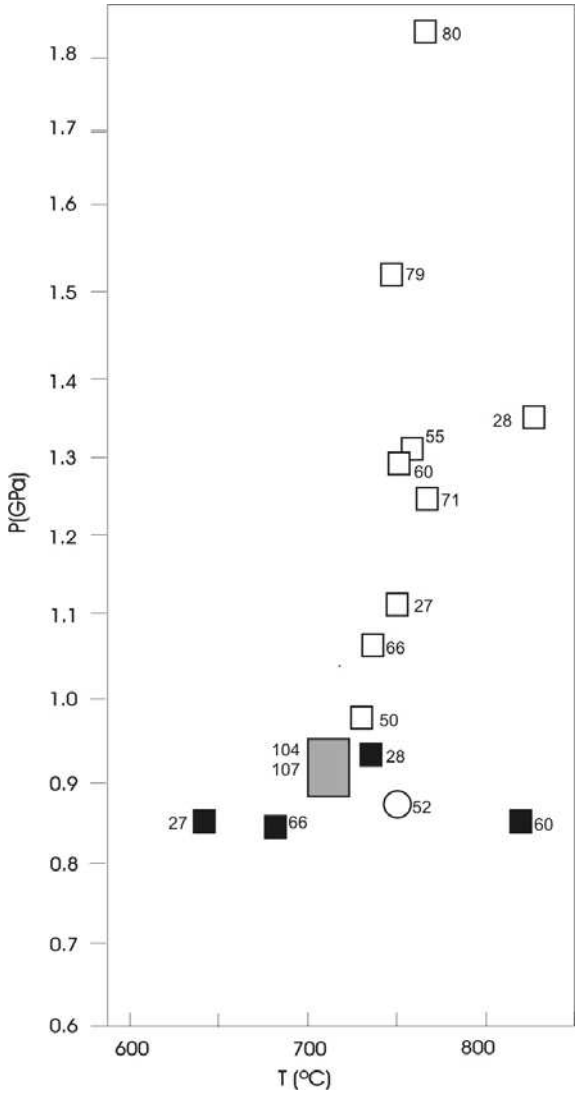

Fig. 17: Estimated P-T conditions for mafic rocks of the GFTZ with potential P-T paths: white squares: P-T estimates from Cpx-Grt-Pl-Qtz assemblages; black squares: P-T estimates from Opx-Grt-Pl-Qtz assemblages; white dot: P-T estimate from a meta-aluminous gneiss of the hanging wall of the Dorval detachment; grey rectangle: P-T estimates from Hbl-Grt-Pl-Qtz assemblages.

Based upon these determinations, the distribution of P-T estimates (Fig. 17) indicates a potential pressure drop of over 500 MPa for a temperature decrease of about 100ºC. This is in keeping with a quasi-isothermal decompression path in the granulite slab. As noted above it is likely that this path extends into a major temperature drop (isobaric cooling) as attested by the quenching of retrograde reactions. It should be noted that the lowest P-T

conditions recorded by the mafic assemblages are at the lower limit of the stability field of kyanite, whereas the ubiquitous Al-silicate in nearby aluminous layers is sillimanite (Indares and Martignole, 1989b), an indication for the more efficient compositional readjustment to varying P-T conditions in metaluminous rocks.

12. 4. Conditions in the hanging wall of the Dorval detachement

The hanging wall of the Dorval detachment belongs to the amphibolite grade Reservoir Dozois Terrane (Indares and Martignole, 1990). The occasional presence of kyanite together with sillimanite in aluminous layers and the absence of metamorphic orthopyroxene in the mafic rocks of this terrane constrain P-T conditions to about 750ºC and 750 MPa. In the immediate vicinity of the Dorval detachment, estimations with the Cpx-Grt thermometer and the Pl-Cpx-Grt-Qtz barometer (sample 51) yield peak conditions of 735ºC and 1100 MPa, whereas Opx-bearing assemblages suggest isothermal pressure reequilibration at 968 MPa, both estimates being within the kyanite field. Nearby garnet-sillimanite gneisses give, for the same temperature, a pressure estimate of 900 MPa (sample 52, Fig. 17).

The persistence of Grt-Qtz assemblages along most of the section across the GFTZ probably means that following decompression and unroofing, cooling was too rapid for pervasive back-reaction. Back-reactions seem to be more efficient in the southeastern part of the GFTZ, just underneath the Dorval detachment, where unroofing was probably less pronounced and cooling less rapid, allowing the Grt-Qtz-producing retrograde reactions to proceed.

13. Tectonic implications

A section accross the GFTZ in western Quebec reveals the presence of a steep metamorphic gradient, in part resulting from NW-directed thrusting (or SE-directed underthrusting) as attested by the presence of high-grade rocks preferentially on the hanging walls of the faults. The most striking example of this tectonic activity is provided

by granulites overriding sillimanite-muscovite schists along the McLaurin thrust. Extensional displacement along SE-diping faults is also well represented in the GFTZ, but the persistance of higher-grade rocks on the hanging wall of the faults shows that it does not reach the same magnitude as contractional tectonics. The reverse situation prevails along the southeastern boundary of the GFTZ, the hanging wall of which is made of amphibolite grade rocks. This boundary is thus considered as a detachment (Dorval detachment) that played a major role in the exhumation of the GFTZ.

Estimated pressures for the GFTZ attest to burial of the actual level of exposure at depths in excess of 35 km. Considering the present crustal thickness of over 40 km in this area (Martignole et al., 2000) and assuming that no underplating occurred, a double crust was probably built immediately to the southeast of the Grenville Front just before 1 Ga.

The reconstruction of the metamorphic P-T history suggests that peak pressure conditions as high as 1.4 GPa were followed by a major, near-isothermal, pressure drop of over 0.4 GPa (i.e. over 10 km) probably followed by relatively fast (isobaric?) cooling. Such a scenario accounts for the preservation of close to thermal peak mineral compositions and to simultaneous closure of the various isotopic systems. On the other hand, it implies a very efficient process in order to achieve a major pressure reduction in a relatively short time. As contractional tectonic dominates the GFTZ, extension along the Dorval detachment is thus considered as the mechanism that led to the exhumation (pressure decrease) and high cooling rates (quenching of mineral compositions and isotopic systems) of high-grade rocks of the GFTZ.

The rapid exhumation of high-pressure terranes is well documented in eclogite domains, usually associated with oceanic subduction, a mechanism that does not apply to the GFTZ, because there is no evidence for oceanic closure preceding the 1 Ga high-pressure metamorphism. More recently, tectonic extrusion of lower crustal levels along basement ramps has been proposed as an alternative mechanism for the exhumation of eclogitic rocks (Indares et al., 2000). Although the GFTZ with its basal thrust and upper décollement

apparently behaved as an extruded slab, the close connection between the hypabyssal Mesoproterozoic dykes of the foreland and their granulitic or eclogitic equivalents southeast of the Front, precludes major horizontal displacement as expected in an extruded slab. If extrusion is a viable process for the emplacement of high-pressure allochthons (HP belt of Rivers et al., 2002) it does not adequately account for the exhumation of high-pressure granulites in the parautochthon. A different scenario has to be envisaged for the GFTZ according to which crustal thickening resulted in a major gravitational instability SE of the Grenville Front, thus triggering the formation of a high relief. In the absence of a coeval foreland basin on Laurentia, the resorption of this relief was most likely achieved by tectonic erosion, in the form of unroofing by extensional collapse. Among the structure that may be responsible for tectonic erosion the main one is the SE-dipping Dorval detachment that could be envisaged as the logical isostatic response to the ca. 1 Ga-old crustal thickening (synconvergent extension?). In this case, exhumation of high-pressure granulites is related to an essentially vertical, gravity-controlled tectonics.

Current models for the 1.0 Ga contractional tectonics along the Grenville Front invoque thrusting toward the foreland in an outward propagating convergent orogen (e.g. Beaumont et al., 1992; Beaumont and Quinlan, 1994). This tectonics post-dates the emplacement of allochthons, some of which also contributed to the exhumation of high-pressure rocks (Rivers et al., 2002). In both cases, crustal thickening results from piling up of crustal unit in a NW-directed displacement, a process that is limited by the flexural elasticity of the underlying Archean lithosphere and by the simultaneous action of gravity. An alternative scenario, designed to take into account these limitations and the continental-scale crustal thickening along the Grenville Front, is based on the onset of an intracontinental, SE-dipping subduction zone, such as the one that may be presently operating in Pamir and may be along some sections of the northern edge of the Tibetan plateau (Martignole, in review).

14. Conlusions

1) Major and trace element analyses of mafic dykes and pods from the GFTZ show that these units are the metamorphosed equivalents of Paleoproterozoic and Mesoproterozoic diabases and associated rocks from the Grenville foreland.

2) Evidence for emplacement at upper to mid-crustal level of these mafic rocks (chilled margins; magmatic layering; olivine relicts) combined with cross-cutting relationships of high-grade fabrics of the gneisses by the mafic rocks provide compelling evidence for a pre-Grenvillian (late Archean or Paleoproterozoic?) exhumation of the area now located SE of the Genville Front.

3) Available geochronological data, supported by new U-Th-Pb age determinations on monazite, have failed to identify any thermal perturbation between about 2.6 Ga and 1.0 Ga. In particular, no evidence was found for the magmatic activity and metamorphism reported in the Ontario section of the GFTZ at 1.47-1.45 Ga (Davidson and van Breemen, 1994).

4) Geobarometric and geothermometric determinations on suitable assemblages from the mafic rocks considered to have undergone a single metamorphic event yield pressure estimates in excess of 1.2 GPa, with potential peak above 1.5 GPa, for average temperatures of 800°C, attesting to a burial of the GFTZ at depths in excess of 35 km. Data provided by mineral reactions in prograde and retrograde coronas suggest a steep, hair pin type, clockwise P-T loop that implies high geothermal gradients, deep burial and dramatic decompression, unexpected in an intracontinental deformation zone.

5) The high-pressure rocks exhumed SE of the Grenville Front have younger metamorphic ages (ca. 1.0 Ga) than those from the high-pressure rocks emplaced at the leading edge of the Grenvillian allochthons (ca. 1.04 Ga; Rivers et al., 2002). Their mode of exhumation is in fact fundamentally different: vertical uplift following crustal doubling in the first case, tectonic extrusion in the second.

6) Finally, the Grenville Front rather than the limit of NW-directed thrusting may be considered as a zone of plate-scale underthrusting that may account for abnormal depths of burial in an intracontinental deformation zone.

References

Avramtchev, L., LeBel-Drolet, S., 1981. Catalogue des Gîtes minéraux du Québec: Région de l'Abitibi. Ministère de l'Énergie et des Ressources naturelles du Québec, DPV 7-44.

Beaumont, C., Quinlan, G., 1994. A geodynamic framework for interpreting crustal-scale seismic reflectivity patterns in compressional orogens. Geophysical Journal International 116, 754-783.

Beaumont, C., Quinlan, G., Hamilton, J., Willet, S., 1992. Preliminary results from a mechanical model of the tectonics of compressive crustal deformation. Alberta Basement Transects. LITHOPROBE Workshop Report 28, 22-61.

Berman, R.G., 1988. Internally consistent thermodynamic data for minerals in the system Na_2O-MgO-FeO-Fe_2O_3-Al_2O_3-SiO_2-TiO_2-H_2O-CO_2. Journal of Petrology 29, 445-522.

Berman, R.G., 1991. TWQ version 1.02. Geological Survey of Canada, Website.

Berman, R., Aranovitch, L.Ya., 1996. Optimized standard state and solution properties of minerals. I. Model calibration for olivine, orthopyroxene, cordierite, garnet and ilmenite in the system FeO-MgO-CaO-Al_2O_3-TiO_2-SiO_2. Contributions to Mineralogy and Petrology 126, 1-24.

Berman, R.G., Aranovitch, L.Ya., Pattison, D.R.M., 1995. Reassesment of the garnet-clinopyroxene Fe-Mg exchange thermometer: II. Thermodynamic analysis. Contributions to Mineralogy and Petrology 119, 30-42.

Bethune, K.M., 1997. The Sudbury dyke swarm and its bearing on the tectonic development of the Grenville Front, Ontario, Canada. Precambrian Research 85, 117-146.

Bethune, K.M., Davidson, A., 1997. Grenvillian metamorphism of the Sudbury diabase dyke-swarm: from protolith to two-pyroxene garnet coronite. Canadian Mineralogist 35, 1191-1220.

Buchan, K.L., Mortensen, J.K., Card, K.D., 1993. Northeast-striking Early Proterozoic dykes of southern Superior Province: multiple episodes of emplacement recognized from integrated paleomagnetism and U-Pb geochronology. Canadian Journal of Earth Sciences 30**,** 1286-1296.

Davidson, A., van Breemen, O., 1994. U-Pb ages of granites near the Grenville Front, Ontario. Radiogenic age and Isotopic Studies: Report 8. Geological Survey of Canada, Current Research 1994-F, 107-114.

Childe, F., Doig, R., Gariepy, C., 1993. Monazite as a metamorphic chronometer, south of the Grenville Front, western Quebec. Canadian Journal of Earth Sciences 30**,** 1056-1065.

Dickin, A.P., McNutt, R.H., Marcantonio, F., Martignole, J., 1989. The SW Grenville Province as a reworked Superior Penokean margin. Geological Association of Canada, Program with Abstracts 12, p. 72.

Doig, R., 1979. Rb-Sr geochronology and evolution of the Grenville Province in northwest Quebec. Geological Society of America Bulletin 88**,** 1843-1856.

Dudás, F.Ő., Davidson, A., Bethune, K.M., 1994. Age of the Sudbury diabase dykes and their metamorphism in the Grenville Province. Radiogenic age and isotopic studies: Report 8. Geological Survey of Canada, Current Research 1994-F, 97-106.

Ernst, R., Bell, K., 1992. Petrology of the Great Abitibi Dyke, Superior Province, Canada. Journal of Petrology 33, 423-469.

Ernst, R., Bell, K., Ranalli, G., Halls, H., 1987. The Great Abitibi Dyke, southeastern Superior Provine, Canada . In: Halls, H.C., Fahrig, W. (Eds.), Mafic Dyke swarms. Geological Association of Canada Special Paper 34, 123-135.

Fuhrmann, M.L., Lindsley, D.H., 1988. Ternary feldspar modeling and thermometry. American Mineralogist 73, 201-215.

Gariépy, C., Verner, D., Doig, R., 1990. Dating Archean metamorphic minerals southeast of the Grenville Front, western Québec, using Pb isotopes. Geology 18, 1078-1081.

Girard, R., Moorhead, J., 1994. Géologie de la région de Press-Clova: phase 2 de 3 et 3 de 3. Ministère des Ressources naturelles, Québec, MB 94-34, 40p.

Goncalves, P., Nicollet, C., Lardeaux, J.M., 2003. Finite Strain Pattern in Andriamena unit (North-Central Madagascar): Evidence for Late Neoproterozoic-Cambrian Thrusting during Continental Convergence. Precambrian Research 123, 135-157.

Heaman, L.M., 1989. U-Pb dating of mafic dyke swarms: what are the options? International Association of Volcanology and Chemistry of the Earth's Interior general

assembly, Program with Abstracts, New Mexico Bureau of Mines and Mineral Resources Bulletin 131, p. 125.

Indares, A., 1993. Eclogitized gabbros from the eastern Grenville Province: textures, metamorphic context, and implications. Canadian Journal of Earth Sciences 30, 159-173.

Indares, A., Dunning, G., 1997. Coronitic metagabbro and eclogite from the Grenville Province of western Quebec: interpretation of U-Pb geochronology and metamorphism. Canadian Journal of Earth Sciences 34, 891-901.

Indares, A., Martignole, J., 1989a. The Grenville Front south of Val-d'Or. Tectonophysics 157, 221-239.

Indares, A., Martignole, J., 1989b. The Montréal-Val-d'Or Geotraverse. Geological Association of Canada, Montréal, Guide Book, Fieldtrip A2, 52p.

Indares, A., Martignole, J., 1990. Metamorphic constraints on the evolution of the gneisses from the parautochthonous and allochthonous polycyclic belts, Grenville Province, western Quebec. Canadian Journal of Earth Sciences 27, 357-370.

Indares, A., Rivers, T., 1995. Textures, metamorphic reactions and thermobarometry of eclogitized metagabbros: a Proterozoic example. European Journal of Mineralogy 7, 43-56.

Ketchum, J.W.F., Davidson, A., 2000. Crustal architecture and tectonic assembly of the Central gneiss Belt, southwestern Grenville Province, Canada: a new interpretation. Candian Journal of Earth Sciences 37, 217-234.

Kretz, R., 1983. Symbols for rock forming minerals. American Mineralogist 68, 277-279.

Krogh, T.E., 1994. Precise U-Pb ages from Grenvillian and pre-Grenvillian thrusting of Proterozoic and Archean metamorphic assemblages in the Grenville Front tectonic zone, Canada. Tectonics 13, 963-982.

Krogh, T.E., Corfu, F., Davis, D.W., Dunning, G.R., Heaman, L.M., Kamo, S.L., Machado, N., Greenough, J.D., Nakamura, E., 1987. Precise U-Pb Isotopic Ages of Diabase Dykes and Mafic to Ultramafic Rocks Using Trace Amounts of Baddeleyite and Zircon. In: Halls, H.C., Fahrig, W. (Eds.), Mafic Dyke swarms. Geological Association of Canada Special Paper 34, 147-152.

Kuehner, S.M., Green, D.H., 1986. High-pressure studies of mafic dykes: Implications for the crustal history of the East Antarctic shield. Australian Geological Convention, 8th, Abstracts 15, 215.

Mader, U., Berman, R.G., 1992. Amphibole thermometry : a thermodynamic approach. Current Research, Part E, Geological Survey of Canada, Paper 92-1E, 393-400.

Mader, U., Percival, J., Berman, R.G., 1994. Thermobarometry of garnet-clinopyroxene granulites from the Kapuskasing structural zone. Canadian Journal of Earth Sciences 31, 1134-1145.

Martignole, J., 2003. The Grenville Front as a limit of intracontinental subduction. Geology (in review).

Martignole, J., Friedman, R., 1998. Geochronological constraints on the last stages terrane assembly in the central part of the Grenville Province. Precambrian Research 92, 145-164.

Martignole, J., Pouget, P., 1994. A two-stage emplacement for the Cabonga allochthon (central part of the Grenville Province): evidence for orthogonal and oblique collision during the Grenville orogeny. Canadian Journal of Earth Sciences 31, 1714-1726.

Martignole, J., Reynolds, P., 1997. $^{40}Ar/^{39}Ar$ thermochronometry along a western Quebec transect of the Grenville Province, Canada. Journal of Metamorphic Geology 15, 283-296.

Martignole, J., Calvert, A., Friedman, R., Reynolds, P., 2000. Crustal evolution along a seismic section across the Grenville Province (western Quebec). Canadian Journal of Earth Sciences 37, 291-306.

Montel, J.M., Foret, S., Veschambre, M., Nicollet, C., Provost, A., 1996. Electron microprobe dating of monazite. Chemical Geology 131, 37-53.

Mottana, A., 1986. Crystal-chemical evaluation of garnet and omphacite microprobe analyses: Its bearing on the classification of eclogites. Lithos 19, 171-186.

Mukhopadhyay, B., Bose, M.K., 1994. Transitional granulite-eclogite facies metamorphism of basic supracrustal rocks in a shear zone complex in the Precambrian shield of south India. Mineralogical Magazine 58, 97-118.

Pattison, D.R.M., 2003. Petrogenetic significance of orthopyroxene-free garnet + clinopyroxene + plagioclase ± quartz-bearing metabasites with respect to the amphibolite and granulite facies. Journal of Metamorphic Geology 21, 21-34.

Philippe, S., Gariepy, C., Doig, R., Childe, F., 1990. U-Pb geochronology of late Archean monazites, south of the Grenville Front, western Quebec. Lithoprobe Abitibi-Grenville project, Workshop, Abstracts, p. 18.

Rivers, T., Martignole, J., Gower, C.J., Davidson, T., 1989. New tectonic divisions of the Grenville Province. Tectonics 8**,** 63-84.

Rivers, T., Ketchum, J., Indares, A., Hynes, A., 2002. The High-Pressure belt in the Grenville Province: architecture, timing and exhumation. Canadian Journal of Earth Sciences 39**,** 867-893.

Rushmer, T., 1991. Partial melting of two amphiboles: contrasting experimental results under fluid-absent conditions. Contributions to Mineralogy and Petrology 107, 41-59.

Springer, W., Seck, H.A., 1997. Partial fusion of basic granulites at 5 to 15 kbar: implications for the origin of TTG magmas. Contributions to Mineralogy and Petrology 127, 30-45.

Spear, F.S., 1993. Metamorphic phase equilibria and Pressure-Temperature-Time Paths. Mineralogical Society of America, Monograph Series, Washington, 799 p.

Wynne-Edwards, H.R., 1972. The Grenville Province. In: Price, R.A., Douglas, R.J.W. (Eds),Variations in tectonic style in Canada.Geological Association of Canada Special Paper 11, 927-953.

Table 2: Chemical composition of mafic dykes from the gftz in western Québec

	Group 1									Group 2			
Sample	28	29	59	63	65	104	106	107	108	51	72	80	105
SiO_2	52.07	53.59	51.58	58.20	52.07	51.84	51.54	51.75	51.93	48.51	44.77	43.86	46.41
TiO_2	1.16	0.98	0.72	0.71	0.65	0.61	0.64	0.51	0.81	2.16	2.93	3.91	2.67
Al_2O_3	15.06	15.00	19.24	18.25	14.86	14.19	14.43	14.83	13.86	13.84	15.48	15.30	12.23
Fe_2O_3	11.83	10.73	8.44	6.91	10.66	11.33	10.86	10.75	13.14	16.44	16.54	18.09	19.71
MnO	0.18	0.17	0.13	0.13	0.17	0.19	0.18	0.18	0.21	0.23	0.21	0.22	0.26
MgO	7.21	6.37	5.64	3.15	7.67	8.26	7.79	8.28	7.38	5.92	6.50	5.24	6.11
CaO	9.82	9.94	10.49	5.67	11.46	11.87	11.66	12.02	10.86	9.46	8.09	7.21	8.98
Na_2O	2.29	2.78	3.23	5.15	1.88	1.74	1.72	1.73	1.72	2.89	3.36	4.05	2.45
K_2O	0.65	0.73	0.53	1.18	0.45	0.40	0.45	0.35	0.51	0.93	0.94	1.29	1.20
P_2O_5	0.12	0.11	0.07	0.33	0.07	0.06	0.07	0.05	0.08	0.33	0.63	0.95	0.40
Cr_2O_3	0.03	0.02	0.02	0.01	0.03	0.03	0.03	0.03	0.02	0.02	0.01	0.00	0.02
Total	100.42	100.42	100.09	99.69	99.97	100.52	99.36	100.48	100.52	100.73	99.46	100.13	100.44
Rb	16.0	17.5	11.0	15.2	15.5	17.0	16.3	15.0	21.8	19.8	15.4	22.0	30.9
Sr	265.7	263.6	332.6	1539.0	135.8	108.9	110.9	111.3	115.4	245.5	416.0	383.0	199.2
Y	22.6	21.3	15.5	13.3	18.2	23.8	24.5	22.0	27.6	34.6	37.5	49.6	45.3
Zr	84.9	81.1	47.2	177.7	48.0	31.1	35.0	23.7	45.4	150.4	181.7	301.1	207.7
Nb	7.8	7.8	6.4	1.4	5.1	6.6	7.2	6.7	6.4	11.1	11.0	16.8	12.3
Ni	100.0	53.0	74.0	27.0	106.0	124.0	115.0	124.0	102.0	57.0	79.0	50.0	57.0
V	230.0	220.0	160.0	135.0	209.0	243.0	241.0	229.0	275.0	320.0	249.0	215.0	352.0
Ga	18.5	17.5	17.0	22.4	15.8	12.4	12.8	12.4	13.3	22.3	21.4	20.1	19.4
Pb	3.5	4.3	2.6	10.4	7.0	1.0	1.7	0.4	2.2	7.2	10.4	9.0	5.0
Th	1.5	1.6	<d/l	<d/l	1.0	0.9	1.2	0.6	0.4	3.3	4.8	6.4	<d/l
U	<d/l	<d/l	<d/l	<d/l	<d/l	2.2	2.2	2.3	2.1	<d/l	<d/l	1.6	1.3
X_{Mg}	0.55	0.54	0.6	0.47	0.59	0.59	0.59	0.6	0.53	0.42	0.44	0.37	0.38
Quartz	8.86	8.89	3.32	8.32	9.13	8.77	9.30	8.31	11.20	4.82	0.00	0.00	5.30
Zircon	0.02	0.02	0.01	0.04	0.01	0.01	0.01	0.00	0.01	0.03	0.04	0.06	0.04
Orthoclase	3.83	4.30	3.13	7.00	2.67	2.36	2.68	2.07	3.01	5.47	5.59	7.62	7.09
Albite	19.30	23.43	27.31	43.71	15.92	14.65	14.65	14.57	14.48	24.28	28.59	34.22	20.70
Anorthite	28.79	26.20	36.42	23.34	30.80	29.59	30.53	31.53	28.45	21.90	24.53	19.75	18.80
Diopside	12.22	15.25	10.33	1.00	18.77	21.22	20.06	20.62	17.69	12.52	1.90	0.00	10.76
Hypersthene	12.22	8.74	9.25	7.41	10.41	10.64	10.23	10.97	10.09	8.84	11.55	2.53	10.21
Olivine	0.00	0.00	0.00	0.00	0.00	0.00	0.00	0.00	0.00	0.00	2.70	7.36	0.00
Chromite	0.07	0.05	0.03	0.02	0.06	0.07	0.07	0.06	0.05	0.05	0.02	0.01	0.04
Hematite	11.78	10.69	8.43	6.93	10.67	11.27	10.93	10.70	13.07	16.33	16.63	18.07	19.68
Ilmenite	0.37	0.35	0.30	0.28	0.37	0.39	0.38	0.39	0.45	0.48	0.47	0.50	0.00
Sphene	2.36	1.93	1.38	1.40	1.12	0.99	1.08	0.74	1.40	4.64	6.61	6.99	6.55
Rutile	0.00	0.00	0.00	0.00	0.00	0.00	0.00	0.00	0.00	0.00	0.00	0.80	0.00
Apatite	0.29	0.25	0.18	0.80	0.16	0.15	0.16	0.13	0.18	0.77	1.51	2.25	0.96

Table 3: Chemical composition of selected minerals from mafic dykes

Table 3: Representative garnet compositions

Group	1											2				3
Sample	27	27	28	28	55	60	60	66	66	104	107	51	71	79	80	52
Analysis	r216	r218	r251	r357a	1b64	r17	r416	r330b	r330h	1.3.	1.2.	r341	r326	r18	r133	r11
SiO_2	38.25	38.22	38.16	38.43	38.58	38.13	38.25	38.18	38.00	37.69	38.13	37.33	38.13	37.37	37.62	37.20
TiO_2	0.00	0.01	0.05	0.00	0.00	0.02	0.00	0.00	0.02	0.00	0.02	0.00	0.07	0.01	0.01	0.00
Al_2O_3	21.68	21.79	21.72	21.71	21.63	21.80	21.83	21.88	21.69	21.07	21.47	20.99	21.82	21.11	21.04	21.52
Cr_2O_3	0.00	0.00	0.01	0.00	0.00	0.00	0.03	0.00	0.00	0.00	0.00	0.02	0.01	0.00	0.00	0.04
FeO^T	23.87	24.86	23.71	25.28	23.71	25.10	22.73	24.33	24.37	25.60	21.51	29.34	24.09	29.33	25.48	30.59
MnO	0.96	1.04	0.59	0.77	0.70	1.02	0.69	1.25	1.33	1.36	0.48	1.18	0.59	1.16	1.04	1.20
MgO	7.56	7.50	7.28	7.42	7.48	7.28	7.05	7.75	6.78	5.92	5.73	3.99	7.52	4.46	3.97	7.36
CaO	6.75	6.16	7.74	6.21	7.33	6.61	9.33	6.22	7.15	7.24	11.89	6.55	7.42	5.55	9.77	1.32
Total	99.12	99.64	99.32	99.88	99.49	100.04	100.00	99.67	99.40	98.98	99.32	99.47	99.73	99.03	99.00	99.30
Si	2.978	2.970	2.968	2.980	2.990	2.959	2.957	2.962	2.968	2.980	2.973	2.981	2.957	2.986	2.989	2.947
Ti	0.000	0.001	0.003	0.000	0.000	0.001	0.000	0.000	0.001	0.000	0.001	0.000	0.004	0.001	0.001	0.000
Al	1.990	1.996	1.991	1.984	1.976	1.994	1.989	2.001	1.997	1.964	1.973	1.975	1.994	1.988	1.970	2.009
Cr	0.000	0.000	0.001	0.000	0.000	0.000	0.002	0.000	0.000	0.000	0.000	0.001	0.001	0.000	0.000	0.003
Fe^{3+}	0.032	0.034	0.037	0.036	0.034	0.046	0.052	0.037	0.035	0.057	0.054	0.043	0.045	0.026	0.040	0.041
Fe^{2+}	1.523	1.582	1.505	1.604	1.503	1.584	1.417	1.542	1.557	1.636	1.349	1.916	1.518	1.935	1.653	1.985
Mn	0.063	0.069	0.039	0.051	0.046	0.067	0.045	0.082	0.088	0.091	0.032	0.080	0.039	0.079	0.070	0.081
Mg	0.878	0.869	0.844	0.858	0.864	0.842	0.813	0.896	0.789	0.698	0.666	0.475	0.869	0.531	0.470	0.869
Ca	0.563	0.513	0.645	0.516	0.609	0.550	0.773	0.517	0.598	0.613	0.993	0.560	0.617	0.475	0.832	0.112
TOTAL	8.027	8.032	8.033	8.028	8.022	8.043	8.048	8.037	8.033	8.038	8.040	8.031	8.042	8.020	8.025	8.047
X_{Alm}	0.50	0.52	0.50	0.53	0.50	0.52	0.47	0.51	0.51	0.54	0.44	0.63	0.50	0.64	0.55	0.65
X_{Prp}	0.29	0.29	0.28	0.28	0.29	0.28	0.27	0.30	0.26	0.23	0.22	0.16	0.29	0.18	0.16	0.29
X_{Grs}	0.17	0.15	0.19	0.15	0.18	0.16	0.23	0.15	0.18	0.17	0.30	0.16	0.18	0.14	0.25	0.02
X_{Sps}	0.02	0.02	0.01	0.02	0.02	0.02	0.01	0.03	0.03	0.03	0.01	0.03	0.01	0.03	0.02	0.03

Structural formulae calculated on the basis of 12(O);FeO^T : total Fe as FeO; for analytical techniques, see text.

Table 3 (cont.): Representative plagioclase compositions

Group	1															3
Sample	27	27	28	28	55	60	60	66	66	104	104	107	51	71	80	52
Analysis	r29	r212	r248	r353	r156	r215	r421	r329	r330	a1	a311	b5	r335	r328 2	r143	r12
SiO_2	57.31	51.95	58.61	56.22	57.70	48.94	55.58	54.67	47.20	51.37	55.63	51.34	60.01	58.65	64.51	62.21
Al_2O_3	26.65	30.31	26.15	27.26	26.18	33.60	28.62	28.62	33.33	30.71	28.00	30.45	24.61	26.82	22.00	24.11
FeO	0.05	0.14	0.06	0.29	0.11	0.28	0.04	0.07	0.31	0.09	0.10	0.12	0.16	0.05	0.24	0.02
CaO	8.75	13.11	8.28	9.67	8.25	15.71	10.38	11.22	16.91	13.60	10.14	13.39	6.59	8.12	3.37	4.82
Na_2O	6.20	3.78	6.61	5.71	6.70	2.36	5.40	4.95	1.79	3.70	5.53	3.74	7.59	6.81	9.60	8.49
K_2O	0.41	0.18	0.41	0.32	0.22	0.11	0.23	0.31	0.07	0.17	0.26	0.18	0.38	0.35	0.35	0.38
Total	99.37	99.47	100.12	99.47	99.16	101.00	100.25	99.84	99.61	99.64	99.66	99.22	99.34	100.80	100.07	100.03
Si	2.58	2.37	2.62	2.54	2.60	2.22	2.49	2.47	2.18	2.34	2.51	2.35	2.69	2.60	2.85	2.75
Al	1.42	1.63	1.38	1.45	1.39	1.79	1.51	1.52	1.81	1.65	1.49	1.64	1.30	1.40	1.14	1.26
Fe^{3+}	0.00	0.01	0.00	0.01	0.00	0.01	0.00	0.00	0.01	0.00	0.00	0.00	0.01	0.00	0.01	0.00
Ca	0.42	0.64	0.40	0.47	0.40	0.76	0.50	0.54	0.84	0.66	0.49	0.66	0.32	0.39	0.16	0.23
Na	0.54	0.33	0.57	0.50	0.59	0.21	0.47	0.43	0.16	0.33	0.48	0.33	0.66	0.59	0.82	0.73
K	0.02	0.01	0.02	0.02	0.01	0.01	0.01	0.02	0.00	0.01	0.02	0.01	0.02	0.02	0.02	0.02
Total	4.99	4.99	4.99	4.99	5.00	4.99	4.99	4.99	5.00	5.00	4.99	5.00	5.00	5.00	5.00	4.99
X_{Ab}	0.55	0.34	0.58	0.51	0.59	0.21	0.48	0.44	0.16	0.33	0.49	0.33	0.66	0.59	0.82	0.74
X_{An}	0.43	0.65	0.40	0.47	0.40	0.78	0.51	0.55	0.84	0.66	0.50	0.66	0.32	0.39	0.16	0.23

Structural formulae calculated on the basis of 8(O); for analytical techniques, see text.

Table 3 (cont.): Representative clinopyroxene compositions

Group	1					2		
sample	27	28	55	60	66	51	71	79
Anal.	r310	r242	r1c27	r48	r329	r331	r314	r154
SiO_2	53.36	53.10	51.91	52.18	53.23	52.28	52.71	51.26
TiO_2	0.13	0.37	0.11	0.18	0.11	0.07	0.15	0.53
Al_2O_3	1.69	1.70	2.19	2.14	1.66	1.51	1.65	3.52
Cr_2O_3	0.10	0.03	0.05	0.02	0.06	0.05	0.04	0.00
FeO^T	6.84	7.94	7.96	7.95	7.20	12.87	7.90	14.25
MnO	0.15	0.07	0.13	0.16	0.17	0.19	0.07	0.20
MgO	14.49	14.26	13.92	14.28	14.27	11.63	14.45	10.48
CaO	22.05	22.38	22.55	22.82	22.10	21.13	22.53	18.08
Na_2O	0.37	0.36	0.41	0.40	0.39	0.58	0.34	1.98
Total	99.22	100.22	99.38	100.33	99.21	100.41	100.00	100.52
Si	1.983	1.966	1.939	1.930	1.982	1.969	1.955	1.921
Ti	0.004	0.010	0.003	0.005	0.003	0.002	0.004	0.015
Al	0.074	0.074	0.096	0.093	0.073	0.067	0.072	0.156
Cr	0.003	0.001	0.002	0.001	0.002	0.002	0.001	0.000
Fe^{3+}	0.000	0.000	0.049	0.066	0.000	0.033	0.036	0.099
Fe^{2+}	0.213	0.246	0.200	0.180	0.224	0.373	0.209	0.348
Mn	0.005	0.002	0.004	0.005	0.005	0.006	0.002	0.006
Mg	0.803	0.787	0.775	0.787	0.792	0.653	0.799	0.586
Ca	0.878	0.888	0.902	0.904	0.882	0.853	0.895	0.726
Na	0.027	0.026	0.030	0.029	0.028	0.042	0.024	0.144
Total	3.990	4.000	4.016	4.022	3.992	4.011	4.012	4.040
X_{Jd}	0.03	0.03	0.03	0.03	0.03	0.04	0.03	0.13
X_{cats}	0.02	0.01	0.03	0.03	0.02	0.01	0.02	0.00
X_{Mg}	0.79	0.76	0.80	0.81	0.78	0.64	0.79	0.63

Structural formulae calculated on the basis of 6(O);
FeOT : total Fe as FeO; XMg = Mg/(Mg+Fe^{2+}); for analytical techniques, see text.

Table 3 (cont): Representative orthopyroxene compositions

Group				2
sample	27	28	66	51
Anal.	r312	r342 3	r327	r322
SiO_2	51.81	51.62	51.85	50.12
TiO_2	0.07	0.07	0.04	0.06
Al_2O_3	1.38	1.25	1.71	0.85
Cr_2O_3	0.01	0.00	0.01	0.02
FeO^T	23.32	24.74	22.48	33.37
MnO	0.29	0.26	0.40	0.45
MgO	22.67	21.62	23.03	15.64
CaO	0.45	0.39	0.42	0.51
Na_2O	0.00	0.01	0.02	0.01
Total	100.14	100.08	100.09	101.09
Si	0.963	0.967	0.961	0.969
Ti	0.001	0.001	0.001	0.001
Al	0.030	0.028	0.037	0.019
Cr	0.000	0.000	0.000	0.000
Fe^{3+}	0.044	0.040	0.039	0.043
Fe^{2+}	0.318	0.348	0.309	0.497
Mn	0.005	0.004	0.006	0.007
Mg	0.628	0.604	0.637	0.451
Ca	0.009	0.008	0.008	0.011
Na	0.000	0.000	0.001	0.000
TOTAL	2.015	2.013	2.013	2.015
X_{Mg}	0.66	0.63	0.67	0.48

Structural formulae calculated on the basis of 3(O);
FeOT : total Fe as FeO; XMg = Mg/(Mg+Fe^{2+}); for analytical techniques, see text.

Table 3 (cont.): Representative amphibole compositions

Group	1			2	
sample	28	104	107	79	80
Anal.	r322	H1	H3	r37	r39
SiO_2	43.44	41.31	44.66	40.05	39.08
TiO_2	1.99	0.35	0.94	3.08	3.47
Al_2O_3	12.04	14.94	11.10	12.68	14.27
Cr_2O_3	0.03	0.04	0.05	0.01	0.01
FeO^T	11.91	14.30	12.64	18.24	16.20
MnO	0.05	0.07	0.07	0.09	0.11
MgO	12.41	11.57	13.67	8.55	9.02
CaO	11.82	11.76	11.86	10.54	10.52
Na_2O	1.28	1.54	1.29	2.99	3.11
K_2O	1.41	1.77	1.14	1.30	1.47
Total	96.38	97.65	97.42	97.53	97.24
F	0.01	0.18	0.00	0.02	0.07
Cl	0.12	0.03	0.02	0.03	0.19
Si	6.748	6.434	6.866	6.397	6.215
Ti	0.232	0.041	0.109	0.370	0.415
Al^{IV}	1.600	1.914	1.482	1.951	2.133
Al^{VI}	0.605	0.829	0.530	0.435	0.542
Cr	0.004	0.005	0.006	0.002	0.001
Fe^{3+}	1.232	1.562	1.518	1.280	1.225
Fe^{2+}	0.315	0.301	0.107	1.157	0.929
Mn	0.007	0.009	0.010	0.012	0.014
Mg	2.873	2.686	3.132	2.037	2.138
Ca	1.967	1.962	1.953	1.804	1.792
Na(A)	0.278	0.000	0.270	0.668	0.705
Na(M4)	0.107	0.466	0.115	0.258	0.253
K	0.28	0.351	0.224	0.298	0.265
TOTAL	16.248	16.560	16.322	16.669	16.627
XMg	0.90	0.90	0.97	0.64	0.70
Na+K(A	0.558	0.351	0.494	0.966	0.970

Structural formulae calculated on the basis of 24(O);FeO^T : total Fe as FeO;XMg = $Mg/(Mg+Fe^{2+})$; for analytical techniques, see text.

Table 4: Summary of representative P-T conditions in the mafic dykes

Sample	Reaction	Garnet	Orthopyroxene	Clinopyroxene	Plagioclase	Temperature, °C	Pressure, MPa
S27	(R1), (R3)	r216		r310	r29	750	1115
	(R2), (R4)	r218	r312		r12	641	855
S28	(R1), (R3)	r251		r242	r248	828	1351
	(R2)	r353	r342		r353	734	937
S51	(R1), (R3)	r341		r331	r335	730	980
	(R2), (R4)	idem	r322		idem	730	980
S55	(R1), (R3)	rb64		r1c27	r156	759	1311
S60	(R1), (R3)	r416		r48	r421	748	1300
		r17	r213		r215	820	852
S66	(R1), (R3)	r330h		66r329	66r329	737	1065
	(R2), (R4)	r330b	r327		r330	681	847
S71	(R1), (R3)	r326		r314	r328	766	1248
S79		r18		r15	r12	748	1519
S80	(R1), (R3)	r133		r134	r143	767	1818
S52	GASP	r11			r12	750	876

R1, R2, R/, et R4 sont sujets a changement a la fin

(1) = Cpx-Grt, 2) = Cpx-Grt-Pl-Qtz (3) = Opx-Grt 4) = Opx-Grt-Pl-Qtz (5) = Pl-Grt-Ky-Qtz